Conference paper

Kamil Skonieczny^a, Eli M. Espinoza^b, James B. Derr, Maryann Morales, Jillian M. Clinton^c, Bing Xia and Valentine I. Vullev*

Biomimetic and bioinspired molecular electrets. How to make them and why does the established peptide chemistry not always work?

https://doi.org/10.1515/pac-2019-0111

Abstract: "Biomimetic" and "bioinspired" define different aspects of the impacts that biology exerts on science and engineering. Biomimicking improves the understanding of how living systems work, and builds tools for bioinspired endeavors. Biological inspiration takes ideas from biology and implements them in unorthodox manners, exceeding what nature offers. Molecular electrets, i.e. systems with ordered electric dipoles, are key for advancing charge-transfer (CT) science and engineering. Protein helices and their biomimetic analogues, based on synthetic polypeptides, are the best-known molecular electrets. The inability of native polypeptide backbones to efficiently mediate long-range CT, however, limits their utility. Bioinspired molecular electrets based on anthranilamides can overcome the limitations of their biological and biomimetic counterparts. Polypeptide helices are easy to synthesize using established automated protocols. These protocols, however, fail to produce even short anthranilamide oligomers. For making anthranilamides, the residues are introduced as their nitrobenzoic-acid derivatives, and the oligomers are built from their C- to their N-termini via amide-coupling and nitro-reduction steps. The stringent requirements for these reduction and coupling steps pose non-trivial challenges, such as high selectivity, quantitative yields, and fast completion under mild conditions. Addressing these challenges will provide access to bioinspired molecular electrets essential for organic electronics and energy conversion.

Keywords: bioinspired; biomimetic; electrets; NICE-2018; peptide synthesis; selective reduction.

Introduction

In the context of *biomimetics* and *biological inspiration*, this publication describes the development of molecular electrets and focuses on the synthetic challenges for making their bioinspired analogues (Fig. 1).

Article note: A collection of invited papers based on presentations at the 4th International Conference on Bioinspired and Biobased Chemistry & Materials (NICE-2018), Nice, France, 14–17 October 2018.

Kamil Skonieczny: Department of Bioengineering, University of California, Riverside, CA 92521, USA; and Institute of Organic Chemistry, Polish Academy of Sciences, Kasprzaka 44-52, 01-224 Warsaw, Poland

Eli M. Espinoza and Maryann Morales: Department of Chemistry, University of California, Riverside, CA 92521, USA

James B. Derr: Department of Biochemistry, University of California, Riverside, CA 92521, USA

Jillian M. Clinton: Department of Bioengineering, University of California, Riverside, CA 92521, USA

Bing Xia: GlaxoSmithKline, 200 Cambridgepark Dr., Cambridge, MA 02140, USA

© 2019 IUPAC & De Gruyter. This work is licensed under a Creative Commons Attribution-NonCommercial-NoDerivatives 4.0 International License. For more information, please visit: http://creativecommons.org/licenses/by-nc-nd/4.0/

^aPresent address: College of Chemistry, University of California, Berkeley, CA 94720, USA.

^bPresent address: College of Bioengineering, University of California, Berkeley, CA 94720, USA.

Present address: Division of Chemistry and Chemical Engineering, California Institute of Technology, Pasadena, CA 921125, USA.

^{*}Corresponding author: Valentine I. Vullev, Department of Bioengineering, University of California, Riverside, CA 92521, USA; Department of Chemistry, University of California, Riverside, CA 92521, USA; Department of Biochemistry, University of California, Riverside, CA 92521, USA; and Materials Science and Engineering Program, University of California, Riverside, CA 92521, USA, e-mail: vullev@gmail.com

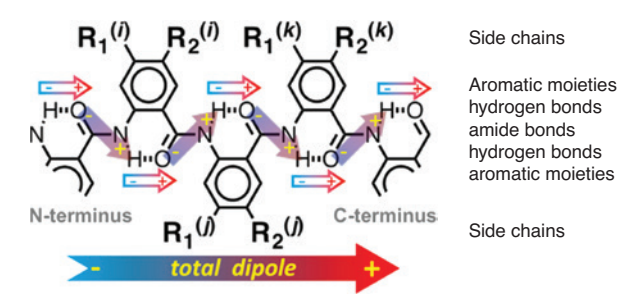


Fig. 1: Bioinspired molecular electrets, composed of Aa residues, showing (1) the origin of the macrodipole, i.e. the total electric dipole, from amide and hydrogen bonds, ordered in the center along the backbone, (2) the aromatic moieties providing sites for electron or hole transfer, and (3) the side chains, R₁ and R₂, modulating the electronic and optical properties of the residues.

(Electrets are systems with ordered electric dipoles, i.e. they are the electrostatic analogues of magnets [1].) Description of multi-step syntheses of electret oligomers illustrates the improvements needed for making their preparation facile and accessible for the broad research and development community. Fundamental research in experimental and theoretical physical chemistry leads to the breakthroughs demonstrating the broad impact of biomimetic and bioinspired structures on a myriad of fields, such as materials engineering, energy conversion and electronics. It is, however, the ability to prepare such structures that makes this line of research and development even possible.

Charge transfer (CT) is one the most important processes for sustaining life as we know it. CT not only drives vital processes in living systems such as cell respiration and photosynthesis, but also ensures the efficient performance of materials and devices essential for modern life [2–7].

Biology provides a wide range of invaluable paradigms for advances in all areas of science and engineering. Deepening and expanding the understanding of how living systems work by *mimicking* them, and implementing this knowledge in unorthodox manners as defined by *biological inspiration*, illustrates the broad impacts that the transitions from *biomimetic* to *bioinspired* approaches have [1, 8]. Transformative developments in understanding and implementing CT benefit immensely from the numerous robust examples found in biological redox and energy-conversion systems.

While "biomimetic" and "bioinspired" approaches commenced as key tools for science and engineering, through the last couple decades, they evolved into independent research fields. The term "biomimetic" appeared in the early 1970s, mostly in the context of developing synthetic procedures [9–12]. It did not take long to spread to other areas of science and engineering [13–15]. Concurrently, references to "biological inspiration" in computer engineering and medicine in the 1940s and 1960s, respectively [16, 17], predate the "biomimetic" terminology. The use of the term "bioinspired," however, took off in the early 1990s [18–23], as the next step forward to broad utilization of biological concepts.

The evolution of the fields of biomimetics and biological inspiration has important impacts on the CT science and engineering. Dye-sensitized solar cells, artificial photosynthesis, enzymatic fuel cells, and solar fuels are some of the concepts that originated from understanding and implementing biological concepts in CT systems [24–32].

Electric dipoles are ubiquitous and their localized fields present largely underutilized paradigms for controlling CT, the importance of which cannot be overstated [5]. The ideas about dipole effects on CT have evolved since the middle of the 20th century [33–35]. The initial work focused on dipoles embedded in proteins, i.e. on biological electrets.

With intrinsic dipoles of up to 5 Debye per residue, protein helices are the best-known molecular electrets [36–38]. Therefore, their biomimetic analogues, i.e. synthetic polypeptide helices of alpha amino acids, have been almost exclusively the choice for studying how electric dipoles affect CT [38–43]. However, unless cofactors or residues with redox-accessible side chains are present, proteins and their polypeptide analogues mediate CT via tunneling, limiting the practicality of its efficiency to about 2 nm [44–46]. In photosynthesis,

on the other hand, arrays of cofactors effectively mediate CT over several nanometers via electron hopping [2]. Similarly, hole hopping along the electron-rich bases of DNA and PNA macromolecules allows for efficient CT at record-long distances [47–49].

Combining the structural motifs of protein helices, responsible for the intrinsic macrodipoles, with the concepts of biological arrays that mediate long-range CT, we developed bioinspired molecular electrets based on anthranilamide (Aa) structures (Fig. 1) [1, 50-54]. Similar to protein helices, ordered amide and hydrogen bonds generate macrodipoles along the backbones of the Aa oligomers. Unlike proteins and synthetic polypeptide helices, however, aromatic moieties, directly linked with amide bonds, provide sites for electron or hole hopping that are essential for attaining long-range CT.

Unlike the native α-amino acids, which have single side chains, the Aa residues have two side chains (R₁ and R₂, Fig. 1) presenting another advantage of the bioinspired structures. Variations in these two side chains, permits a broad adjustment of the electronic and optical properties of the Aa residues. Altering between alkyl, alkyloxy and amine side chains varies the Aa reduction potentials over a span of one volt [55–57]. Furthermore, we determined that not only the mesomeric and inductive characteristics of R, and R, but also their exact position, govern the electronic properties of the Aa residues. Moving the same substituent from R, and R, changes the reduction potentials with about 100-200 mV, and results in tens of nm shifts in the optical spectra [55, 56]. In addition to regulating the electronic properties of the aromatic residues, the side chains R, and R, also provide a means for improving the solubility of the Aa oligomers and controlling their self-assembly properties. This role of the side chains is closely related to the functions of the side chains of native amino acids in the formation of tertiary and quaternary protein structures.

While the first report on Aa oligomers came out more than an century ago [58], less than a couple of dozen publications on these aromatic oligoamides have appeared since then [59-69]. The studies of Aa oligomers have focused on their structural features, including their ability to serve as rigid templates for foldamers and templates with biological activity [68–72]. Recently, our analysis of the electronic properties of different Aa oligomers demonstrated for the first time, theoretically and experimentally, that they are molecular electrets [50, 51]. That is, Aa oligomers possess large intrinsic electric dipoles originating from the ordered arrangements of their amide and hydrogen bonds [50]. We also determined that without side chains, i.e. R = R = H (Fig. 1), the Aa oligomers have a high propensity for aggregation [51], which may decrease the enthusiasm for their use as "well-behaved" structural motifs as reflected by the limited number of publications. Because the Aa conjugates are polypeptides, we developed a set of electron-rich non-native Aa residues as building blocks for hole-transfer molecular electrets [53, 55–57, 73–75]. Using alkyl-containing substituents as side chains, especially as R₂ (Fig. 1), dramatically increases the solubility of the Aa residues in organic solvents and prevents their aggregation [56]. Attaching electron-deficient chromophores to them allowed us to demonstrate that even a single Aa residue can substantially rectify CT [52, 54].

The Aa conjugates are oligopeptides. Thus, it appears that with all available well-established robust protocols for polypeptide synthesis, making Aa oligomers should be trivially easy. For more than 100 years, peptide chemistry has evolved with huge amount of manpower involved in its development [76–85]. Several important breakthroughs in the second half of the 20th century led to the current state-of-the-art solid-phase peptide synthesis (SPPS) protocols that are readily automatable, allowing facile preparation of 50-residue polypeptides in a few days [86–90]. The polypeptides are built from their C- to their N-termini on a solid support. Each amino acid is introduced as free carboxylates with orthogonal protections of their amine and the side-chain groups (if needed). *In situ* activation of the carboxylates allows them to couple to the terminal free amines on the solid support. Amine deprotection of the amine of the coupled residue prepares it for the coupling with the next amino acid. Quantitative yields of each coupling and deprotection step ensure that the product cleaved from the solid support can be readily purified using preparative and semi-preparative HPLC [89].

Despite all the advances in peptide chemistry, however, none of these synthetic protocols are applicable for making Aa oligomers. First, the anthranilic residues are considerably less reactive than aliphatic amino acids. The carbonyls at the *ortho*-position decrease the nucleophilicity of the free amines. Similarly, the protected *ortho*-amines decrease the electrophilicity of the carbonyl carbons of the activated carboxylates. Second and most important, activation of carboxyl groups at the *ortho* position to amides or protected amines leads to the formation of stable cyclic structures that cannot react with the aromatic free amines on the oligomer termini and suppress any further coupling all together [64].

Introducing each of the Aa residues as its 2-nitrobenzoic acid analogue addresses both issues. The strongly electron-withdrawing nitro group increases the electrophilicity of the carbonyl carbon. In addition, the nitro group does not react with the neighboring activated carboxylates to form stable structures that terminate the coupling step. Hence, Aa oligomers are synthesized from their C- to N-termini via a sequence of amide coupling and nitro-group-reduction steps [51, 64]. Despite the large number of procedures for selective reduction of nitro groups to amines [91–94], in the context of the synthesis of Aa oligomers, this step presents key challenges. It is a six-electron six-proton reduction proceeding through three intermediates. Reducing conditions that lead to complete conversion of nitro groups to amines under mild conditions, without affecting the rest of the Aa oligomer, are not quite routine.

Herein, after a brief review of biomimetics and biological inspiration, we introduce the concept of CT molecular electrets based on motifs derived from biology, i.e. dipoles originating from ordered amide and hydrogen bonds. The century of development of synthetic bioorganic chemistry produced robust and reliable tools for making biomimetic electrets based on polypeptide α -helices, which unfortunately are not truly useful for the preparation of bioinspired Aa structures. Introducing the amines as nitro groups presents an alternative strategy for making Aa oligomers. Based on this approach, we demonstrate the synthesis of Aa dimer, trimer and tetramer composed of electron-rich residue, 4Pip (Fig. 2). The reduction steps essential for converting the N-terminal nitro groups into amines present some of the key challenges. We show that few of the "established" procedures for nitro reduction are feasible for Aa synthesis. Our findings demonstrate that Cr (II) in organic media provides the best means for selective reduction of a nitro-Aa derivative to the corresponding amine. Electrochemical and spectroscopic analyses of the synthesized oligomers (Fig. 2) reveal key insights about the electronic properties of these aromatic amides.

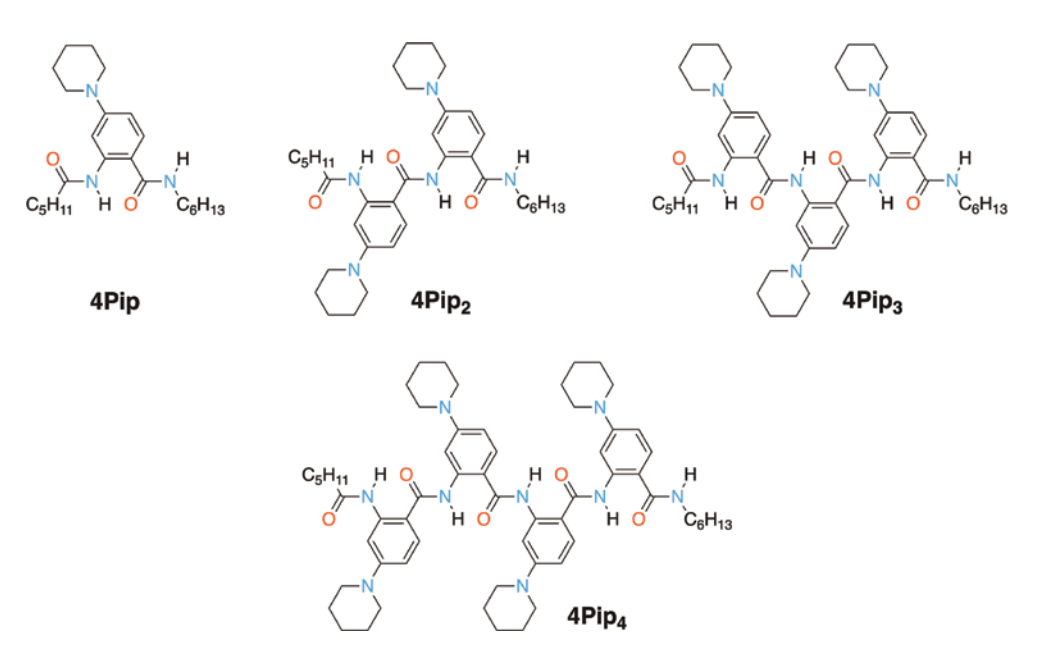


Fig. 2: Bioinspired molecular electret oligomers, composed of an electron-rich residue, 4Pip (R_1 = piperidin-1-yl, R_2 = H, Fig. 1) with alkyl-capped N- and C-terminal amides.

General considerations

Biomimetic vs. bioinspired. What's the difference?

Transitions from biomimetics to biological inspiration illustrate the broadest impacts that biology can have on other areas of science and engineering. Billions of years of evolution on Earth has produced diversity of life forms with multi-scale organization of complex structural features displaying countless functionalities. Myriads of cellular functionalities emerge from specific molecular (self) assemblies. Tissue functionalities emerge from cell differentiation and organization. Organ functionalities emerge from arrangements of tissues and cells with specific properties. Organisms manifest vital functionalities that emerge from the synergy between the comprising organs. Social organizations of single-cell and multicellular organisms lead to the emergence of new properties and group behavior that the analyses of the individual participants cannot predict [95]. Such structure-function relationships at multiple spatial and temporal scales still remain not only challenging for engineers to achieve, but also far from completely understood by mathematicians, physicist, chemists, biologists and social scientists.

While biomimicry merely imitates structural features of living systems, biomimesis aims at attaining the functionality of biological entities by copying their structures [1, 8]. Hence, the biomimetic approaches are indispensable for unveiling how biology works, and for discovering important structure-function relationships in living systems by employing maquettes that are often less complex than the copied biological counterparts. Furthermore, systematic lowering of the complexity of the maquettes of the examined biological systems reveals which parameters are important for attaining certain functionalities of interest.

As engineering tools, biomimicry and biomimesis provide a direct means interfacing synthetic materials and biomedical devices with living tissue [96, 97], where the interests are not only in biocompatibility, but also in biofunctionality [98]. A two-way relationship between biology and engineering has been the principal driving force behind the development of the whole field of microfluidics [99-101]. Mimicking features of the cardiovascular system leads to sophisticated microfluidic designs. Concurrently, microfluidic devices provide indispensable platforms for studying living cells and tissues under natural conditions outside the complexity of the living organisms, which frequently leads to key discoveries in biology and medicine [102-104].

While biology offers a myriad of lessons for advanced engineering, a direct implementation of biological and biomimetic structures is far from optimal for materials, devices and other manmade systems targeting similar functionalities. To achieve reasonable lifespans, for example, living systems rely on damage management via numerous self-repair mechanisms that evolved through the thousands of millennia [105–110]. That is, damages are inevitable. Hence, deviating a small portion of the life energy for driving self-repair processes ensures longevity. Conversely, engineered self-repair approaches of abiotic systems are still immensely far from what life can do. Therefore, the longevity of manmade systems relies on damage prevention. It involves over-engineering in order to decrease the probability of damages to occur. While such over-engineering cannot completely prevent damages, it still increases the lifespans of devices and other manmade structures.

Biological and biomimetic structures are frequently quite less than optimal for engineering solutions. Therefore, *biological inspiration* provides routes for overcoming the inherent limitations of the living systems. Bioinspired approaches involve taking ideas and elements from biology and implementing them in manners different from their natural occurrence [1, 111–113]. For example, materials genome has nothing to do with DNA or other information-carrying biomolecules. Instead, materials genome encompasses biologically inspired extraction of specific structural information from huge databases for guiding the experimental development of new materials with specific targeted functionalities [114–118]. Therefore, a broad range of functionalities that surpass what nature offers can readily emerge from bioinspired approaches.

Overall, biomimetics (encompassing biomimicry and biomimesis) broadens and deepens the understanding of how living systems work, and builds toolkits for biological inspiration. Conversely, biological inspiration leads to countless unexplored possibilities for energy science, electronics, photonics, materials design and numerous other fields of science and engineering.

Molecular electrets based on amide structures

While making small magnets has inherent limitations, making large electrets can prove challenging. The drastic decrease in the Curie temperature (and the Néel temperature) with the decrease in particle size, limits how small molecular magnets can be [119–121]. Conversely, the ease of extracting charges (electrons and ions) from every medium, except vacuum, defines the practical limitations on how large molecular electrets and their dipoles can be. Therefore, bottom-up approaches are the best for pursuing designs of electrets, and especially of molecular electrets, which provide immensely attractive paradigms for nanometer-scale control of CT.

Amide bonds are widespread rigid linkers in biomolecules and synthetic polymers. They are easy to form and possess large permanent electric dipoles [122]. Therefore, amides are an excellent choice as building blocks for molecular electrets [51, 53]. Concurrently, hydrogen-bonding networks are essential for holding together macromolecular secondary conformations and for ensuring that the electric dipoles are ordered. Formation of a hydrogen bond leads to shift of electron density from the negative pole of one dipole (e.g., from the amide oxygens) to the positive poles of another one (e.g. to the amide protons) (Fig. 1). This polarization extends the center the negative charges away from the first dipole and the center of the positive charges away from the second one, increasing the magnitude of both. Therefore, the collective shift of the electron density up on the formation of hydrogen-bonding network in protein helices and Aa oligomers enhances their macrodipoles [50, 123].

In addition to their roles as dipole sources, as covalent linkers, and as hydrogen-bond donors and acceptors, amides can strongly affect the electronic properties of aromatic moieties to which they are directly attached [124]. The mesomeric electron-donating properties of amides when attached via their nitrogens strongly affect the distribution of the frontier orbitals of the Aa residues. Thus, the amide linkers in Aa conjugates define not only the electronic coupling with electron donors and acceptors attached to them, but also their resistance against oxidative degradation during hole transfer processes [55].

Overall, peptide bonds, i.e. carboxyamides, have all the attractive properties for the designs of molecular electrets. The impressive advances in the peptide chemistry should ensure the synthetic procedures for an easy access to a wide variety of molecular structures with large permanent electric dipoles.

Making polypeptides

In ribosomes, the natural synthesis of proteins proceeds from their N- to their C-termini by selectively adding a single amino acid at a time [125]. Catalytic condensation between amines and non-activated carboxylates allows for chemical replication of such biosynthesis of polypeptides [126]. Nevertheless, the best established methods for chemical synthesis of polypeptides build them from their C- to their N-termini [127]. It involves a series of amide-coupling steps between the N-terminal free amines of a peptide and the activated carboxylates of the amino acids that is the next in the sequence. To ensure the selectivity of this reaction, the amine of the added amino acid is protected and the polypeptide with the free amine does not have free carboxylates that can be potentially activated. Therefore, amine deprotection follows each amide coupling step. That is, the synthesis of a polypeptide with *n* residues requires 2*n* reaction steps. For reasonable amounts of the final polypeptide products, each of these steps has to undergo with a quantitative yield.

Since the first report of dipeptide synthesis in 1901 [76], peptide chemistry has evolved with exponential rates. It involved important breakthroughs, especially during the second half the 20th century, such as (1) the discovery of Boc and Fmoc protection groups, along with the protection groups with orthogonal sensitivity for the side-chain functional groups of the native amino acids [87, 88, 128-130]; (2) the development of a wide range of reagents for mild in situ activation of amino-acid carboxylates for amide coupling [131, 132]; (3) the development of SPPS and the automated fast Boc and Fmoc protocols [86, 133–137], recognized by the 1984 Nobel Prize in Chemistry, awarded to R. B. Merrifield; (4) the development of resins for SPPS with different sensitivity toward acidic cleavage, i.e. allowing the use of anything from HF to weakly acidic organic solution as cleavage reagent, and producing polypeptides with different C-termini, i.e. free carboxylates and primary amides [138]; and (5) the development of preparative reverse phase HPLC for facile purification of peptides from SPPS.

The interest in the field drove the involvement of an enormous number of researchers in its development. Following the chemical synthesis of oxytocin, reported in the 1953 [77], teams led by Panayotis Katsoyannis at University of Pittsburgh and by Helmut Zahn at RWTH Aachen University independently reported the synthesis of insulin [79, 80]. Concurrently, collaborative work involving teams from Academia Sinica, Shanghai, and Peking University also led to the total chemical synthesis of insulin, the activity of which was confirmed using animal studies [81, 83]. These demonstrations of obtaining biologically active polypeptides via a chemical means provided important motivation for perfecting and further developing the procedures for peptide synthesis.

The current protocols for SPPS are readily prone to automation for expedient preparation of polypeptides that are more than 50-residue long. While protein expression, using the machinery of living cells, allows for making long sequences exceeding tens of kDa, chemical peptide synthesis provides the means for facile incorporation of synthetic amino acids and other moieties into the polypeptide backbone [139–145], which is a key advantage in the exploration of new non-native structures essential for bioinspired science and engineering. For the Fmoc protocol, for example, each residue is introduced as a free-carboxylate derivative with Fmoc protected amine that is to be added to the polypeptide backbone, and acid-sensitive protection of the side-chain functional groups. The in situ activation of the carboxylate allows it to be coupled to the free amines (or hydroxyls) on the resin solid support. Traditionally, activating the carboxylates as halides provides the reactivity needed for the amide coupling. Acid chlorides are considerably more reactive than acid fluorides. This high reactivity, however, makes the chlorides more prone to causing side reactions, and thus, acid fluorides have made their way into the modern SPPS [131, 132]. After all, the fluoride is the smallest possible leaving group for amide coupling reactions rendering acid fluorides quite desirable when steric hindrance is an issue.

Conversely, the sensitivity to moisture renders the utility of acid halides for peptide synthesis. Therefore, activating the carboxylates to form intermediates that are considerably more susceptible to nitrogen nucleophiles, rather than oxygen ones, have become the preferred route for SPPS. Carbodiimides, such as DCC, EDC and DIC, readily react with carboxylic acids under mild conditions (the presence of a base is not required) to form *O*- or *N*-acylisoureas. The acylisoureas are inherently unstable and susceptible to nucleophilic substitutions; the produced ureas are excellent leaving groups. Therefore, a huge excess of hydroxyl derivatives, such as N-hydroxysuccinimide (NHS) or 1-hydroxybenzotriazole (HOBt) always accompanies the administration of carbodiimide reagents. Moieties, such as NHS and HOBt form esters that are quite susceptible to nucleophilic attacks from amines (to form amides), while relatively stable in the presence of water and other oxygen nucleophiles. In fact, it is quite common to carry out NHS amide-coupling chemistry in aqueous solutions, and the commercially available HOBt reagent comes as a hydrate, e.g. HOBt · 2 H,O, and used as received.

An alternative for HOBt, 1-hydroxy-7-azabenzotriazole (HOAt), presents routes for further improvements of the yields that is invaluable for difficult amide-coupling steps. The pyridine nitrogen at position 7 in HOAt provides an extra hydrogen-bonding site for stabilizing the transition states with α -amino acids [146]. The use of HOAt instead of HOBt, however, may not necessarily prove beneficial for transition states with different geometries when coupling β - and γ -amino acids, or aminobenzoic acids.

Onium derivatives (i.e. uronium and phosphonium salts) of HOBt and HOAt (such as TBTU, BOP, HATU and PyAOP) encompass another important class of reagents for mild in situ activation of carboxylates that has revolutionized automated SPPS. In the presence of base, these electrophilic onium derivatives readily react with the deprotonated carboxylic acids to form conjugates that are susceptible to nucleophilic attacks in quantitative yields. The added large excess of HOBt or HOAt ensures the formation of the corresponding active esters that have long enough lifetimes to react with the free amines on the solid support. Because carboxylic anhydrides (that are equally good for coupling with the immobilized amines) are another outcome from such activation, the acid should be added in four-fold excess to ensure quantitative yields for the amide coupling. In addition, the molar amounts of some of these onium reagents should not exceed 95 % or 99 % that of the α -amino acid to prevent racemization.

Difficult coupling steps may require heating of the reaction mixtures with the solid support and protocols involving microwave heating are implemented in commercially available peptide synthesizers [147, 148]. Elevated temperatures can address challenges of kinetically impeded reactions, and microwave treatment is particularly useful when the entropic components of the activation energy is the underlying reason for slow conversion rates. While such elevated temperature aid difficult coupling steps, they do not prevent low yields originating from undesired side reactions. In fact, heating may accelerate and even add new side reactions involving not only the reagent solution and the immobilized polypeptide, but also the resin may not be necessarily inert at high temperature.

Because of the dense multiple functionality in a peptide chain, the formation of five or six-member cyclic structures is frequently favored (though undesirable). If certain residues, like glycine and tryptophan, are present in the sequence, base catalyzed hydantoin formation can occur [149]. In some extreme protic conditions (e.g. in the presence of carboxylic acids in high concentrations), undesired six-member ring formation involving two neighboring residues is possible via cleavage of the ester on the C-terminal side of the dimer. The diketopiperazine formation is responsible for losses due to cleaving of the reaction intermediates from the solid support before the completion of the synthesis. Kinetic studies show that proline and valine at the C-terminal are extremely susceptible to this side reaction, especially in the presence of free carboxylic acid in the solution [150]. To avoid such a process, HOBt has to be added in large excess, so that the formation of HOBt ester will be favored over the anhydride formation.

Succinyl and glutaryl derivatives readily form by cyclization between the aspartate and glutamate side chains, respectively, and their α -carboxyl or carboxylamides. Since under the conditions of Fmoc synthesis the carboxyl side chain groups are protected as t-butyl esters, such undesirable cyclization can occur only during the deprotection. Therefore, the cleavage and deprotection times ought not to exceed 2 or 3 h [149].

Also, primary amides in the side chains (e.g. in glutamine and asparagine) are susceptible to dehydration intramolecular reactions with the α -carboxyl group under the conditions of activation with onium reagents [149]. Therefore, the use of acid-sensitive protection groups of the primary amides in the Gln and As n ensures the decrease in the reactivity of these side chains.

Overall, the current SPPS methodologies are practically perfect for facile preparation of polypeptides of α-amino acids that fold to assume helical structures and form biomimetic molecular electrets. Furthermore, robust algorithms with excellent predicting power, along with molecular-mechanics modeling tools, offer a means for reliable selections of *de novo* sequences of α-amino acids that assume helix folds with high probability for various media. Also, the understanding of leucine-zipper interfacing between protein helices provides paradigms in primary sequences that ensure tertiary and quaternary folds of coil-of-coils helix bundles with co-directional orientation of the macrodipoles [151–154].

Results and discussion

Making bioinspired molecular electrets

Bioinspired molecular electrets based on Aa structures are polypeptides (Fig. 1). With the amazing advances in peptide chemistry, it appears that the permeation of Aa oligomers should be immensely facile using automated SPPS protocols. The decades of development of the peptide-synthesis protocols, however, has targeted the preparation of polypeptides of aliphatic α -amino acids. The bioinspired molecular electrets, on the other hand, comprise aromatic β-amino acids (Fig. 1). The structural differences between the Aa conjugates and the derivatives of the native amino acids render the state-of-the-art peptide-synthesis protocols useless for making bioinspired molecular electrets.

The amines and the activated carboxylates of anthranilic conjugates are not as reactive as those of α amino acids. Especially with electron-withdrawing carbonyls at *ortho* position, the aromatic free amines at the N-termini of Aa oligomers are not as nucleophilic as the aliphatic amines of native peptide residues. In addition, the electron-donating (protected) amines compromise the electrophilicity of the activated carboxylates next to them in the aromatic rings.

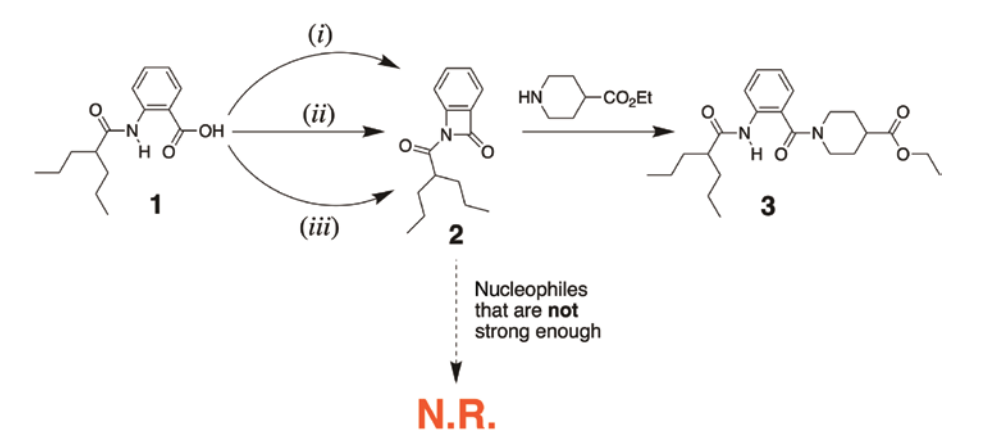
Most importantly, activation of the carboxylate in anthranilic conjugates leads to the formation of stable cyclic intermediates [64]. Similar to the intramolecular cyclization induced by activating the native glutamine and asparagine [149], this condensation upon activation of anthranilic carboxylates suppresses the progress to amide coupling [64].

We observe that treating anthranilamides with different activation reagents (i.e. halogenating, onium and carbodiimide derivatives) lead to the same products that are always a water-molecule lighter than the starting materials as determined using high-resolution mass spectrometry (HRMS). The facile chromatographic isolation of these products proves their stability and allows us to determine that the preferred routes involve intramolecular reaction between the activated carboxylate and the amide or the protected amine next to them to form four-member cyclic lactams (Scheme 1). This finding differs from previous reports for the intermolecular condensation leading to six-member-ring azlactones upon carboxylate activation [64]. Still, the produced four-member-ring lactams are quite stable and can be opened only with strong nucleophiles, such as piperidines (Scheme 1). These findings render even the established peptide-synthesis protocols useless for preparing bioinspired molecular electrets based on anthranilamide structures.

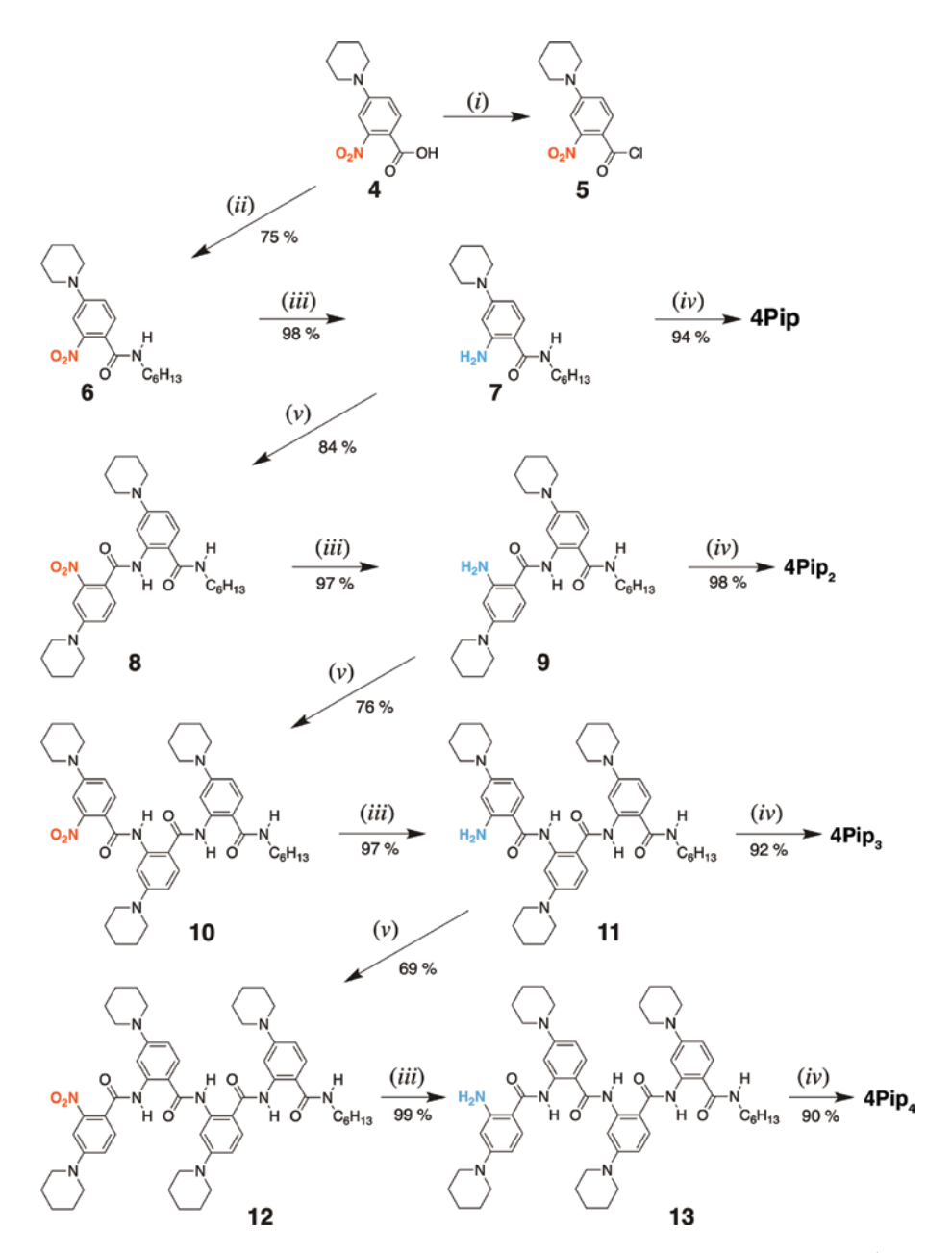
Instead of using anthranilic acids with protected β-amines, introducing each residue as the corresponding derivative of the 2-nitrobenzoic acid (Scheme 2) addresses the grave inherent challenges for making polypeptides based on Aa structures. Thus, in lieu of the established protocols based on amine deprotection, the building of Aa molecular electrets involves a series of amide-coupling and selective nitro-group-reduction steps [51, 64].

To illustrate this concept, we synthesize oligomers of an electron-rich amino-Aa residue, 4Pip (Scheme 2) [56] that, along with its 2-amino derivative, is quite susceptible to oxidative degradation under harsh reaction conditions. Employing chloride activation, along with heterogeneous Pd-catalyzed H, reduction, affords the 4Pip_ oligomers in high yields. Coupling alkyl acids with terminal Aa amines (using anhydride chemistry) proceeds with yields exceeding 90%. Conversely, amide coupling between Aa conjugates (using chloride chemistry) affords yields of about 70-85 % (Scheme 2). While these latter yields are acceptable for solutionphase procedure, they are not sufficient for SPPS.

The reduction steps converting the nitro groups into amines proceed with quantitative yields (Scheme 2), which is quite desirable for making Aa conjugates. The heterogeneous nature of this reduction, however, precludes its utility for solid-phase procedures. Furthermore, H, in the presence of Pd catalyst cleaves most carbon-halogen bonds and reduces certain electron-deficient aromatic compounds.



Scheme 1: Activation of the carboxylates of Aa residues leads to stable cyclic lactams. (i) C,O,Cl., DCM, 3 drops DMF, -78 °C; (ii) EDC, HOBt, NMM, DMF; and (iii) TFFH, NMM, DMF (N.R. = no reaction).



The large variety of coupling procedures developed for SPPS offers many options for improving the synthesis of Aa oligomers. Despite the importance of selective reduction of nitro groups, on the other hand, such procedures for producing amines that are potentially suitable for SPPS are scarce.

Selective reduction of nitro groups in Aa conjugates

The reduction of a nitro group to an amine is a six-electron-six-proton process. It is a sequence of three two-electron-two-proton steps, involving the reduction of nitro to nitroso group, nitroso group to hydroxylamine, and hydroxylamine to amine. Incomplete reduction leaving hydroxylamines along with the amines, followed by amide coupling, leads to a mixture of products that are quite challenging to separate chromatographically. The acylhy-

droxylamine impurities, however, have distinct NMR signals and are readily detectable using HRMS, showing exact mass of the product plus an oxygen atom, which is an indication for incomplete reduction. Consumption of the reducing reagent changes the electrochemical potential of the reaction mixture. To prevent incomplete reduction, therefore, depletion of the reducing reagent should not be allowed, i.e. the reducing reagent should be added in excess in the beginning of the reaction or replenished during the progress of the reaction.

To ensure feasibility for SPPS, reactions for reducing nitro groups to amines should (1) be homogeneous, fast, and highly selective; (2) proceed with quantitative yields in organic solvents (that keep the resin swollen) at room temperature and atmospheric pressure; and (3) not leave any impurities stuck to the solid support, i.e. the resin should be easy to wash with DMF or other organic solvents after each reduction step. To survey the performance of the various reduction methods, we test the reduction of 5-bromo-2-nitro Aa analogue, 14, to the corresponding amine, 15 (Scheme 3). Reaction yields, prevention of debromination, mildness of the conditions (i.e. as close to room temperature as possible), and keeping the reaction solution clear (i.e. no precipitate formation for the duration of the reaction), are the criteria for the feasibility of the reduction method for implementation in SPPS protocols.

Tin (II) chloride dissolved in alcohols or other organic solvents, is one of the most popular reagents for selective reduction of nitro groups to amines [91], and we have successfully used it for the synthesis of Aa derivatives [52]. Elevated temperature is essential for driving this reduction to completion with reasonable rates.

Despite its reported use for solid-phase synthesis [155–157], the need for prolonged heating and the left over insoluble side products render SnCl, impractical for SPPS. While SnCl, has a good solubility in organic solvents and the starting reaction mixtures are clear, the requirement for large amounts of reducing agent (i.e. three Sn²⁺ ions are needed for reducing each nitro group) and the inherent humidity under basic conditions (i.e. the reduction of nitro groups consumes protons and produces water) lead to insoluble tin (IV) and tin (II) conjugates. Our tests with implementing SnCl, for SPPS show that after the first and the second reduction steps, the impurities from tin side products become impossible to remove from the resin, which severely compromises the yields of the synthesized Aa peptide. Furthermore, the conditions of tin (II) reduction cause cleavage of the C-Br bonds.

Carbon monoxide is a good reagent for selective reduction of nitro groups [93]. The need for high pressure or catalysts, however, makes CO nitro reduction somewhat undesirable for SPPS protocols. Conversely, the electrochemical potentials of many metals allow them to selectively reduce nitro groups to amines. The heterogeneous nature of such reduction methods using solid metals, however, renders such approaches unfeasible for solid-phase protocols. Combining carbon monoxide with such metals, at zero oxidation state, presents an alternative. Dicobalt octacarbonyl is soluble in organic solvents and exhibits pronounced selectivity for reduction of nitro groups [158]. We successfully employ Co,(CO), for selective reducing aromatic nitrogroups to the corresponding amines in bromine-containing Aa derivatives (with yields of 75–95%) [8, 54] and in conjugates with electron-deficient chromophores susceptible to reduction (with yields of 60–70 %) [7]. Such reduction with Co,(CO), however, requires elevated temperature and at the end of the reaction, dark-red colored precipitate of side products forms.

Focusing on room-temperature procedures, trichlorosilane appears to present an alternative as a hydrogen-donating reagent for reducing nitro groups to amines [159, 160]. Using HSiCl, allows us to achieve 40 % yield for reducing 14–15. As effective as HSiCl, is as a reducing agent, it is also prone to sol gel polymerization driven by the humidity in the media.

Dithionite ion, $S_2O_4^{2-}$, is another moiety with practically perfect electrochemical potential for selective reduction of nitro groups in molecules with complex functionality at room temperature. Sodium dithionite

Scheme 3: Reduction of a 5-bromo-2-nitro Aa analogue to the corresponding amine at room temperature: (i) HSiCl., DIPEA, MeCN, 0 °C→r.t. (40 %); (ii) Na,S,O,, K,CO,, H,O/heptylviologen, DCM, r.t. (64 %); and (iii) CrCl,, DMF, r.t. (95 %).

is a mild reducing reagent that is widely used in biochemistry and biomaterials science for mild reduction of protein cofactors and for reductive amination [161–163]. While immensely soluble in water, the readily available dithionite salts are insoluble in organic solvents. Also, making organic-soluble dithionite salts without oxidizing them is not truly straightforward [164–166]. Using solid support containing polyethylene glycol (PEG) that swells in water [167], appears as a good alternative. The hydrophobic nature of the Aa oligomers, however, can cause undesirable folds in the hydrogels during the synthesis and prevent the exposure of the nitro groups to the aqueous media with the reducing reagent. Furthermore, the acid-halide amide coupling, which seems to the preferred route for Aa synthesis, is immensely sensitive to moisture in the reaction mixtures, making the regularly used hydrophobic polystyrene resins the preferred solid support for SPPS of bioinspired molecular electrets.

Phase-transfer catalysts (PTCs) allow for addressing the challenges with the $Na_2S_2O_4$ solubility [168, 169]. It involves the implementation of two phases of immiscible liquids: (1) an aqueous solution of the dithionite reducing agent kept at basic pH; and (2) an organic solvent, such as CH_2Cl_2 , in which the nitro compound is dissolved or the swollen resin is kept. Tetrabutylammonium salts with anions that are not soluble in organic solvents, such as SO_4^{2-} , present a good choice for PTC added to the aqueous phase. Ion pairing between N^+ (C_4H_9) $_4$ and $S_2O_4^{2-}$ makes the reducing agent soluble in organic media allowing it to diffuse to the nitro compounds. While it has been successfully used for solid-phase synthetic protocols [170, 171], our tests reveal that this PTC approach does not produce **15** from **14** in acceptable yields.

As an alternative to PTC, the use of an organic-soluble redox couple for shuttling electrons from the dithionate in the aqueous medium to the nitro compound in the organic phase presents an excellent alternative [172]. The electrochemical potential of this redox couple should be right between the reduction potentials of the dithionite and of the targeted nitro group. Benzyl, heptyl and other hydrophobic viologens are an excellent choice for such electron shuttles and they can be successfully employed in solid-phase synthesis [172]. The use of n-heptyl viologen as an electron shuttle produces **15** from **14** with 38 % yields. We observe that an increase in the equivalents of the added viologen from 0.03 to 2.7 improves the yields from 40 % to 64 %.

This finding brings an important point. The reduction potentials of the reaction media should be negative enough to completely reduce the nitro groups to amines, but not too negative to drive the reduction of other functional groups. Therefore, the reducing reagents with best selectivity have potentials that are quite close to those of the nitro groups. Lowering the activity (or the concentration) of the reduced form of the reagent or increasing the activity of its oxidized form can cause a positive shift in its potential just large enough to prevent the reduction of the nitro groups. If the PTC does not maintain the activity of the dithionite in the organic media large enough to ensure the required electrochemical potential for reduction of 14, the reaction cannot proceed to completion. Similarly, the rates of viologen reduction by dithionite and of the nitro-group reduction by the reduced viologen, along with the partition coefficients of these species, control the ratio between the activities of reduced and the oxidized forms of the viologen in the organic media. Our observations show that an increase in the overall viologen concentration favors the reduction of 14, which is consistent with increase in the amount of reduced viologen making the electrochemical potential of the organic media negative enough for the reduction of the nitro group.

Resorting to a different reducing agent, chromium (II), allows us to achieve practically quantitative yields for reducing **14–15** in reasonable times at room temperature. When in organic media, e.g. $CrCl_2$ in DMF, the $Cr^{3+}|Cr^{2+}$ redox couple has the reduction potential to drive the reduction of nitro groups to amines to completion. Furthermore, the sufficient solubility of the chromium compounds in organic solvents makes this reduction procedure implementable in solid-phase synthetic protocols [173]. Unlike $SnCl_2$, $Na_2S_2O_4$, $Co_2(CO)_8$, H_2 and other reducing reagents, however, $CrCl_2$ is kinetically unstable and immensely susceptible to oxidation in air and in other oxygen-containing environment. Therefore, we carry out the reduction of **14–15** by chromium (II) in an argon atmosphere in a glove box where the oxygen level is under 1 ppm. The yields of this reduction exceed 95 % and the washing off the chromium compounds after the completion of the reaction is quite straightforward.

Adding manganese or other solid metals maintains the level of chromium (II) in the reaction mixture [174]. That is, the Cr^{3+} | Cr^{2+} redox couple aids electron shuttling from the solid metal to the nitro compound.

Implementation of this procedure in solid-phase synthesis requires a closed flow system with two reaction vessels, one containing the solid metal and the other – the resin solid support [175]. The reducing metal enriches the solvent of chromium salts in Cr2+, which diffuses or flows to the resin in the other compartment [175].

How does the length of the molecular electrets affect their electronic properties?

All 4Pip conjugates absorb in the UV region of the spectrum (Fig. 3). The increase in the number of residues does not linearly increases the absorptivity. Instead, the bathochromic shifts and the splitting of the absorp-

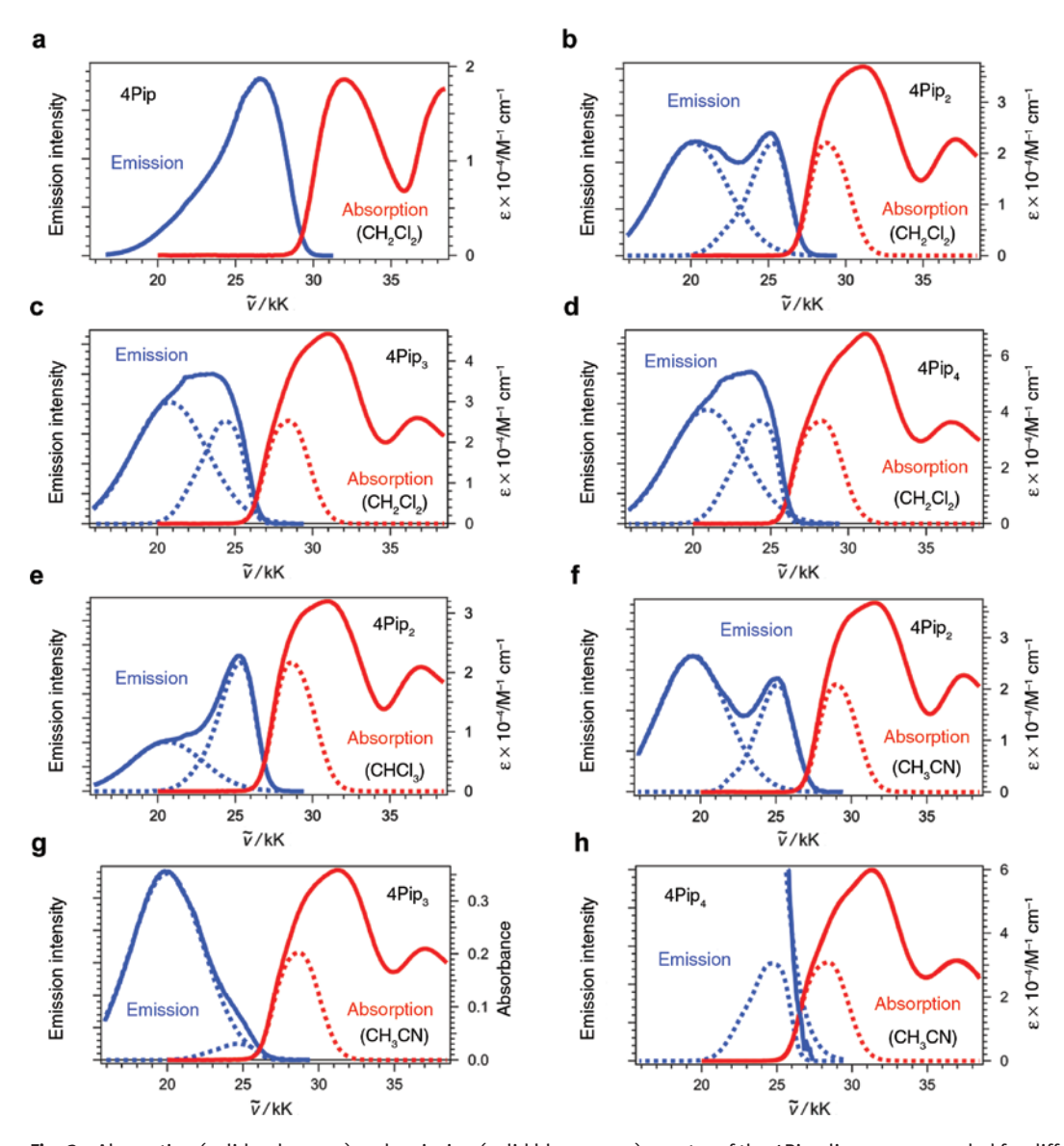


Fig. 3: Absorption (solid red curves) and emission (solid blue curves) spectra of the 4Pip oligomers, recorded for different solvents (λ_{∞} = 330 nm for all oligomers except for the monomer, 4Pip, which is 310 nm). The dotted lines represent the products of deconvolution from fitting the spectral with sums of Gaussians. (a-d) Absorption and emission spectra of (a) 4Pip, (b) 4Pip,, (c) 4Pip, and (d) 4Pip, for CH,Cl,. (e, f) Absorption and emission spectra of 4Pip, for (e) CHCl, and (f) CH,CN. (g, h) Absorption and emission spectra of 4Pip, for CH₂CN: (g) normalized spectral maxima; and (h) normalized deconvoluted components at the crossing spectral edges.

tion bands (as evident from the appearance of shoulders), induced by lengthening of the oligomers (Fig. 3), are consistent with excitonic coupling between the residues.

The emission spectra show similar splitting where the medium polarity and the number of the residues enhance the relative intensity of the low-energy band (Fig. 3). Two principal phenomena can account for these trends: (1) aggregation with increase propensity for long oligomers in polar media; and (2) formation of emissive CT states that cannot be directly accessed from the ground states by direct optical excitation.

Aggregation induced by increased solvent polarity is possible if these polar oligomers assemble in stacks with co-directionally oriented dipoles, e.g. forming H-like aggregates. Increasing the number of residues increases the total magnitude of the dipoles. Concurrently, polar media screen the dipole-generated localized fields responsible for repulsive interaction in the hypothesized assemblies, consistent with observation for similar Aa oligomers with no side chains and different capping moieties of their N- and C-termini ($R_1 = R_2 = H$ Fig. 1) [51]. The identical groups capping the N- and C-termini of the 4Pip oligomers and the lack of concentration dependence in the optical spectra, however, renders the aggregation as an origin of the observed trends (Fig. 3) quite unlikely.

Only for the monomer, 4Pip, in relatively non-polar media, we observe aggregation as the concentration rises to hundreds of μ M (Fig. 4a). For the dimer, trimer and tetramer, variations in sample concentration from nM to mM does not alter the optical spectra (Fig. 4b). While these findings may suggest for immensely small dissociation constants, we cannot exclude other reasons for the observed splits in the spectral bands.

Aromatic alkyl amines have a large propensity for forming excited twisted intramolecular charge-transfer (TICT) states. Theoretical analysis, however, reveals that Aa residues with amines at position 5, i.e. $-R_2 = -NR'R''$, do not form TICT states [52]. Shifting the electron-donating amines from position 5 (R_1) to position 4 (R_2) considerably alters the electronic properties of the Aa residues. Thus, we cannot preclude a propensity of 4Pip conjugates to form TICT states, which polar media should enhance as consistent with the observed trends.

The optical excitation energy, \mathcal{C}_{00} , as expected, decreases with an increase in the length of the oligomers (Table 1). This decrease is most pronounced, by about 0.3 eV, between the monomer and the dimer. A further increase in the oligomer length to a tetramer leads to only about a 0.1-eV decrease in \mathcal{C}_{00} , which is consistent with delocalization of the frontier orbitals limited to about three residues. Specifically, the permanent dipoles elevate the energy levels of the frontier orbitals at the C-termini, and lower those at the N-termini. That is,

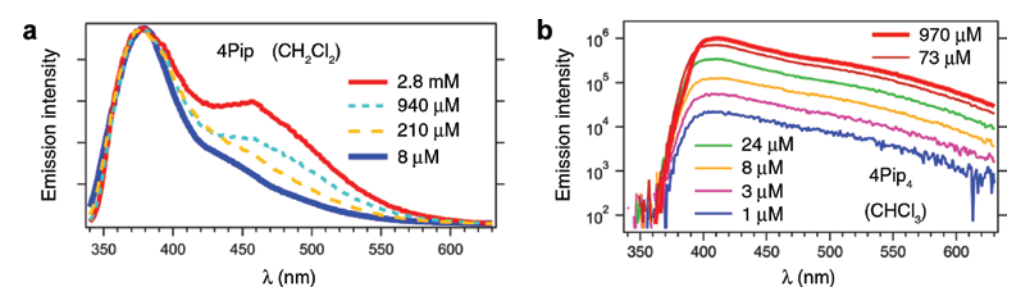


Fig. 4: Concentration dependence of the emission spectra of the 4Pip monomer and tetramer for chlorinated solvents. (a) Normalized spectra presented in a liner intensity scale ($\lambda_{ex} = 310 \text{ nm}$). (b) Spectra presented in a logarithmic intensity scale ($\lambda_{ex} = 330 \text{ nm}$).

Table 1: Excitation energy, $\mathscr{C}_{00}/\text{eV}$, of the 4Pip oligomers for different solvent media.

Solvent	4Pip	4Pip ₂	4Pip ₃	4Pip ₄
CHCl ₃	3.60	3.33	3.26	3.23
CH ₂ Cl ₂	3.61	3.35	3.25	3.22
CH ₃ CN	3.65	3.36	3.28	3.25

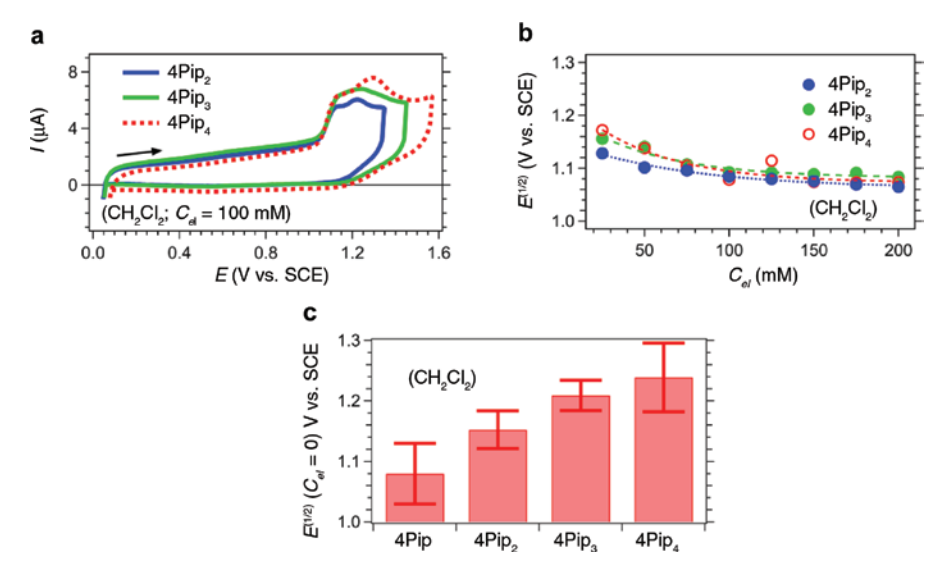


Fig. 5: Electrochemical characteristics of the 4Pip conjugates. (a) Cyclic voltammograms of the dimer, trimer and tetramer for dichloromethane solution in the presence of 100 mM N(n-C, H_0), PF₆ (ν = 50 mV s⁻¹). (b) Dependence of the reduction potentials of oxidation (obtained from the first inflection points of the anodic waves [176]) on the concentation of the supporting electrolyte, C_{cl} [177, 178]. (c) Reduction potentials for the oxidation of the oligomers extrapolated to zero electrolyte concentation.

the HOMOs of the oligomers are located at the C-terminal residues, while the LUMOs – at the N-termini [50]. Increasing the lengths of the oligomers decreases the HOMO-LUMO overlaps and transitions from HOMO to LUMO + n and from LUMO to HOMO-n become characteristic of the observed features in the optical spectra.

Similar to the 4Pip monomer [57], the oligomers of this residue manifest irreversibility during electrochemical oxidation (Fig. 5a), suggesting for the formation of unstable radical cations. Indeed, chemical reversibility of voltammograms guarantees the stability of the oligomers to transfer charges [55]. Lack of reversibility at moderate scan rates, however, does not preclude them from successfully mediating CT in the nanosecond, picosecond and femtosecond time domains. For example, while millisecond oxidative degradation results in irreversible behavior at moderate scan rates, holes residing on a residue for less than a nanosecond during efficient CT will have negligibly short time to initiate relatively slow chemical transformations.

In the presence of supporting electrolyte (0.1 M or more), the oxidation of the oligomers occurs practically at the same potential (Fig. 5a,b), suggesting for a considerable localization of the radical cation under these conditions. Conversely, lowering the electrolyte concentation reveals potentially a size dependence on the propensity of these oligomers to oxidize, as reflected by the positive shift in the reduction potential with the increase in the number of residues (Fig. 5b,c), which could be ascribed to dipole induced impedance of the oxidation. The experimental uncertainty of these changes as revealed by the relatively large error bars (Fig. 5c), however, renders the substantiality of this trend somewhat unfeasible.

Overall, the exciton of the 4Pip oligomers appears to delocalize over two-to-three residues. The radical cation, at least in electrolyte media, is localized on one or a maximum of two Aa residues. These findings suggest that while the amide bonds appear to provide rigidity and partial conjugation along the backbones of the oligomers, they do not ensure broad delocalization of the excitons and the holes on the 4Pip conjugates. The nodes on the carbonyl carbons of the frontier π -orbitals of the amide bonds [124] can be a source for this limitation of the delocalization.

Conclusions

Biomimetic molecular electrets, based on polypeptide helical structure of α -amino acids, are relatively easy to make using automated synthetic protocols. The established procedures for peptide synthesis, however, cannot produce bioinspired anthranilamide electrets. Introducing each residue as the corresponding nitrobenzoicacid derivative places strict demands on the selective reduction of nitro groups to amines. Survey of the broad variety of available reduction methods reveals that only a few such procedures are feasible for Aa synthesis and even fewer are potentially implementable in SPPS. Our findings reveal that viologen²⁺ | viologen⁴⁺ and Cr³⁺ | Cr²⁺ organic-soluble redox couples manifest some of the best electrochemical properties for selective reduction of nitro groups in Aa derivatives. Using these redox couples for shuttling electrons from reducing agents in a different solid or liquid phase offers routes for implementation in solid-phase synthesis protocols. These advances are important steps toward making the bioinspired molecular electrets readily available to wide research and development communities. Furthermore, the optical and electrochemical properties of the anthranilamide oligomers reveal relative localization of the excitons and the holes, i.e. the positive charges, placed on them.

Experimental

Cyclic lactams and opening them (Scheme 1)

2-(2-Propylpentanamido)benzoic acid (1)

Anthranilic acid (397 mg, 2.9 mmol) was placed in a 50 mL and suspended in DCM (3 mL), blanked with continuous flow of N, and placed in a dry ice/acetone bath. While the reaction was mixing 2-propylpentanoic acid (472 µL, 2.76 mmol) was slowly added followed by the dropwise addition of NMM (1 mL, 9 mmol). The reaction mixture was allowed to warm up to room temperature and was stirred overnight. The reaction was then concentrated in vacuo. Hexanes (25 mL) was added to the solution and vortex until a white precipitate formed to afford 137 mg (0.52 mmol, 18 % yield) of white solid of 1. ¹H NMR (600 MHz, CDCl.) δ /ppm: 10.95 (1 H, s), 8.78 (1H, m), 8.14 (1 H, dd, J=7.9, 1.8 Hz), 7.59 (1H, m), 7.11 (1H, m), 2.34 (1H, dt, J=9.6, 4.7 Hz), 1.71 (2H, m), 1.5 (2H, m), 1.37 (4H, m), 0.91 (6H, t, J = 7.2 Hz); ¹³C NMR (150 MHz, CDCl₂) δ /ppm: 175.8, 172.5, 142.00, 135.7, 131.8, 122.6, 120.6, 113.9, 49.5, 35.3, 20.7, 14.0; HRMS (ESI) calcd. for C₁₅H₂₂NO₂ [M+H]⁺ 264.1600, found 264.15985.

7-(2-Propylpentanoyl)-7-azabicyclo[4.2.0]octa-1,3,5-trien-8-one (2)

1 (1 eq.) was suspended in 50 mL dry DCM in a dry argon-purged flask (1 eq), and two drops of N,N-dimethylformamide (DMF) were added. The mixture was cooled in a dry ice/acetone bath and oxalyl chloride (1 eq.) was added dropwise. The mixture was stirred for 3 h and allowed to warm up to room temperature. After removing the solvents under reduced pressure, the crude product was purified by silica chromatography (hexane: ethyl acetate 4:1) to yield 35 mg (0.14 mmol, 83 % yield) or white solid; 'H NMR (400 MHz, CDCl₂) δ /ppm: 8.19 (dd, J=8.0, 1.4 Hz, 1H), 7.81–7.76 (m, 1H), 7.57 (d, J=8.1 Hz, 1H), 7.51–7.46 (m, 1H), 2.70 (tt, J=9.0, 5.5 Hz, 1H), 1.86–1.76 (m, 2H), 1.61 (ddt, J=13.5, 10.1, 5.9 Hz, 2H), 1.41–1.28 (m, 4H), 0.91 (t, J=7.3 Hz, 6H); ¹³C NMR (100 MHz, CDCl₂) δ/ppm: 165.8, 160.1, 146.4, 136.4, 128.4, 128.0, 126.7, 116.9, 45.4, 35.0, 20.6, 14.0; HRMS (ESI) calcd. for $C_{15}H_{20}NO_{2}[M+H]^{+}$ 246.1494, found 246.1478.

Ethyl 1-(2-(2-propylpentanamido)benzoyl)piperidine-4-carboxylate (3)

Piperidine-4-carboxylic acid ethyl ester (1.2 eq.) was added to a solution of 2 (1 eq.) in DCM (50 mL). After the completion of the reaction, the reaction mixture was concentrated under reduced pressure and crystallized from methanol; Yield: 41 mg (93%). White solid; ¹H NMR (400 MHz, CDCl₂) δ /ppm: 8.81 (s, 1H), 8.21 (d, J=8.3 Hz, 1H), 7.43-7.37 (m, 1H), 7.18 (dd, J=7.6, 1.3 Hz, 1H), 7.09 (t, J=7.5 Hz, 1H), 4.74-4.25 (m, 1H), 4.14(q, J=7.1 Hz, 2H), 4.00-3.64 (m, 1H), 3.09 (t, J=10.2 Hz, 2H), 2.57 (tt, J=10.5, 4.0 Hz, 1H), 2.22 (tt, J=9.6, 1.00 Hz, 1.004.9 Hz, 1H), 2.11–1.84 (m, 2H), 1.82–1.68 (m, 2H), 1.70–1.60 (m, 2H), 1.49–1.39 (m, 2H), 1.39–1.28 (m, 4H), 1.25 $(t, J=7.1 \text{ Hz}, 3H), 0.90 (t, J=7.2 \text{ Hz}, 6H); {}^{13}\text{C NMR} (100 \text{ MHz}, \text{CDCl}_2) \delta/\text{ppm}: 174.7, 173.8, 169.2, 136.5, 130.7, 126.9,$ 124.7, 123.5, 123.2, 60.7, 48.6, 40.8, 35.4, 28.3, 20.8, 14.2, 14.1; HRMS (ESI) calcd. for C_{.2}H₂₆N₂O₆ [M+H]⁺ 403.2597, found 403.2574.

Synthesis of 4Pip oligomers (Scheme 2)

2-Nitro-4-(piperidin-1-yl)benzoyl chloride (5) (i, Scheme 2)

The preparation of 2-nitro-4-(piperidin-1-yl)benzoic acid, 4, was previously described [56]. To a solution of 4 (1 eq.) in DCM, placed in a dry argon-filled flask, three drops of DMF were added and the mixture was cooled in a dry ice/acetone bath. Oxalyl chloride (1 eq.) was added dropwise and the mixture was stirred for 3 h. The residual oxalyl chloride was removed by repeatedly concentrating the mixture and resuspending the residue in 3 mL dry DCM. After three resuspension and concentation steps, the crude acid chloride was used in the subsequent step without further purification.

General procedure 1: reduction of nitro compounds to amines (iii, Scheme 2)

The nitro compound (1 eq.) was dissolved in 75 mL of ethyl acetate and reduced at room temperature with hydrogen (1 atm.) on 10 % Pd/C (0.1 eq.) as a catalyst. The conversion of the nitro group to an amine led to the appearance of blue fluorescence and the progress of the reaction was monitored with TLC. Upon completion of the reduction, the solid support with the catalyst was filtered off and the filtrate was evaporated under reduced pressure. The products were purified using recrystallization from hexane solutions.

General procedure 2: amide formation (v, Scheme 2)

To a solution of the amine (1 eq.) in anhydrous DCM (10 mL) was added one drop of dry pyridine and the mixture was cooled in dry ice/acetone bath while purging with argon. A solution of 5 (1 eq.) in 1 mL dry DCM was added slowly and the mixture was stirred until the reaction was completed, as monitored, using TLC. The solution was poured into 1 N HCl and the organic layer was collected, dried over MgSO, and concentrated in vacuo. The product was purified by column chromatography on silica using hexane/ethyl acetate (4:1) as an eluent.

General procedure 3: capping the N-termini as hexanoic amides (iv, Scheme 2)

Under argon, hexanoic anhydride (1 eq.) was added dropwise to a solution of amine (1 eq.) in dry pyridine (4 mL) cooled in an ice bath. The mixture was allowed to warm up, heated to 40 °C, and stirred until the reaction was completed, as monitored using TLC. The solution was poured into 1 N HCl and the organic layer was collected, dried over MgSO, and concentrated in vacuo. The product was purified by column chromatography on silica using hexane/ethyl acetate (4:1) as an eluent.

N-Hexyl-2-nitro-4-(piperidin-1-yl)benzamide (6) and 4Pip

The precursor for the C-terminal residue, 6, and 4Pip have been previously reported [56]. Compound 6 was prepared from in situ activated 4 and 1-aminohexane, and for 4Pip, the general procedure 3 was used.

2-Amino-N-hexyl-4-(piperidin-1-yl)benzamide (7)

Yield: 450 mg (98 %). White solid; 'H NMR (400 MHz, CDCl.) δ 7.18 (CH-CC=O, d, *J* = 8.9 Hz, 1H), 6.25 (CH-C-PIP, dd, J=8.8, 2.2 Hz, 1H), 6.13 (CH-C-NH,, s, 1H), 5.91 (NH, s, 1H), 5.76 (NH,, s, 2H), 3.39-3.33 (m, 2H), 3.25-3.18 (m, 4H), 1.72–1.63 (m, 4H), 1.63–1.52 (m, 4H), 1.41–1.26 (m, 6H), 0.88 (t, J=6.8 Hz, 3H); ¹³C NMR (100 MHz, CDCl₂) δ 169.1, 154.0, 150.5, 128.2, 107.1, 105.0, 102.0, 49.4, 39.5, 31.5, 29.8, 26.7, 25.3, 24.3, 22.6, 14.0; HRMS (ESI) calcd. for $C_{18}H_{29}N_{30}Na$ [M+Na⁺] 326.2203, found 326.2203.

N-Hexyl-2-(2-nitro-4-(piperidin-1-yl)benzamido)-4-(piperidin-1-yl)benzamide (8)

Yield: 190 mg (84 %). Yellow solid; ¹H NMR (400 MHz, CDCl₂) δ 12.29 (s, 1H), 8.38 (s, 1H), 7.60 (d, J=8.7 Hz, 1H), 7.32 (d, J = 9.0 Hz, 1H), 7.23 (d, J = 2.5 Hz, 1H), 7.00 (dd, J = 8.7, 2.6 Hz, 1H), 6.55 (s, 1H), 6.12 (s, 1H), 3.41-3.28(m, 10H), 1.73–1.53 (m, 14H), 1.41–1.27 (m, 6H), 0.88 (t, J = 6.9 Hz, 3H); ¹³C NMR (100 MHz, CDCl₂) δ 169.0, 164.1, 154.0, 152.5, 150.1, 148.9, 141.9, 129.3, 127.6, 120.1, 117.0, 109.6, 108.7, 105.9, 48.8, 39.8, 31.4, 29.5, 26.6, 25.3, 25.1, 24.2, 24.1, 22.5, 14.1, 14.0; HRMS (ESI) calcd. for $C_{30}H_{02}N_5O_{\mu}$ [M+H+] 536.3231, found 536.3221.

2-Amino-N-(2-(hexylcarbamoyl)-5-(piperidin-1-yl)phenyl)-4-(piperidin-1-yl)benzamide (9)

Yield: 115 mg (97%). White solid; ¹H NMR (400 MHz, CDCl₂) δ 12.13 (s, 1H), 8.36 (d, J=2.5 Hz, 1H), 7.65 (d, J=9.0 Hz, 1H), 7.31 (d, J=8.9 Hz, 1H), 6.53 (d, J=8.8 Hz, 1H), 6.37 (dd, J=9.0, 2.2 Hz, 1H), 6.13 (s, 1H), 6.08(s, 1H), 6.01 (s, 2H), 3.39 (dd, J=12.9, 7.1 Hz, 2H), 3.35–3.30 (m, 4H), 3.28–3.23 (m, 4H), 1.75–1.53 (m, 14H), 1.42-1.25 (m, 6H), 0.89 (t, J = 6.9 Hz, 3H); 13 C NMR (100 MHz, CDCl.) δ 169.3, 168.1, 154.1, 151.5, 142.4, 129.4, 127.5, 109.6, 108.3, 107.2, 106.3, 105.6, 101.5, 49.2, 49.0, 39.8, 31.5, 29.6, 26.7, 25.4, 25.3, 24.3, 22.6, 14.0; HRMS (ESI) calcd. for $C_{30}H_{44}N_5O_3[M+H^+]$ 506.3495, found 506.3573.

2-Hexanamido-N-(2-(hexylcarbamoyl)-5-(piperidin-1-yl)phenyl)-4-(piperidin-1-yl)benzamide (4Pip,)

Yield: 21 mg (98%). White solid; ¹H NMR (400 MHz, CDCl₂) δ 12.43 (s, 1H), 11.84 (s, 1H), 8.41 (d, J = 2.1 Hz, 1H), 8.28 (d, J = 2.1 Hz, 1H), 7.77 (d, J = 9.1 Hz, 1H), 7.33 (d, J = 8.9 Hz, 1H), 6.63 (d, J = 8.0 Hz, 1H), 6.54 (d, J = 7.9 Hz, 1H), 6.10 (s, 1H), 3.42–3.38 (m, 2H), 3.38–3.33 (m, 8H), 2.46–2.41 (m, 2H), 1.80–1.54 (m, 16H), 1.40–1.34 (m, 6H), 1.34–1.28 (m, 4H), 0.94–0.84 (m, 6H); ¹³C NMR (100 MHz, CDCl.) δ 172.5, 169.2, 168.1, 154.2, 142.7, 141.9, 128.9, 127.6, 109.4, 108.7, 106.3, 105.3, 48.9, 48.6, 39.9, 38.7, 31.5, 31.4, 29.7, 29.6, 26.7, 25.4, 25.1, 24.4, 24.3, 22.6, 22.5, 14.0, 13.9; HRMS (ESI) calcd for $C_{3c}H_{53}N_5O_3$ [(M+H)+(-H)] 603.4148, found 603.4168.

N-Hexyl-2-(2-(2-nitro-4-(piperidin-1-yl)benzamido)-4-(piperidin-1-yl)benzamido)-4-(piperidin-1-yl) benzamide (10)

Yield: 71 mg (76%). Yellow solid; ¹H NMR (400 MHz, CDCl₂) δ 12.40 (s, 2H), 8.43 (s, 1H), 8.20 (s, 1H), 7.81 (d, J = 9.0 Hz, 1H), 7.62 (d, J = 8.7 Hz, 1H), 7.34 (d, J = 8.4 Hz, 1H), 7.27 (d, J = 2.5 Hz, 1H), 7.00 (dd, J = 8.7, 2.5 Hz, 1H), 6.70 (s, 1H), 6.57 (s, 1H), 6.14 (s, 1H), 3.43-3.28 (m, 14H), 1.75-1.55 (m, 20H), 1.39-1.28 (m, 6H), 0.89 (t, <math>J = 6.9 Hz, 3H); 13 C NMR (101 MHz, CDCl.) δ 169.0, 168.0, 164.3, 152.6, 150.0, 142.7, 141.6, 129.8, 129.0, 127.7, 120.7, 117.1, 109.8, 109.2, 106.9, 105.7, 48.9, 39.9, 31.5, 29.5, 26.7, 25.4, 25.2, 24.3, 24.1, 22.6, 14.0; HRMS (ESI) calcd. for C. H. N.O. $[M + H^{+}]$ 738.4337, found 738.4342.

2-Amino-N-(2-((2-(hexylcarbamoyl)-5-(piperidin-1-yl)phenyl)carbamoyl)-5-(piperidin-1-yl)phenyl)-4-(piperidin-1-yl)benzamide (11)

Yield: 66 mg (97%). White solid; ¹H NMR (400 MHz, CDCl.) δ 12.37 (s, 2H), 8.41 (d, J=2.5 Hz, 1H), 8.30 (d, J=2.5 Hz, 1H), 7.80 (d, J=9.1 Hz, 1H), 7.71 (d, J=9.0 Hz, 1H), 7.32 (d, J=8.9 Hz, 1H), 6.67 (d, J=9.0 Hz, 1H),6.55 (dd, J = 8.7, 1.8 Hz, 1H), 6.34 (d, J = 8.9 Hz, 1H), 6.16 (s, 1H), 6.12 - 6.08 (m, 1H), 3.43 - 3.22 (m, 14H), 1.75 - 1.54(m, 20H), 1.41–1.27 (m, 6H), 0.88 (t, J = 6.9 Hz, 3H); ¹³C NMR (100 MHz, CDCl₂) δ 169.2, 168.2, 168.2, 154.1, 154.0, 151.5, 143.2, 141.8, 129.7, 128.9, 127.6, 109.7, 109.6, 108.8, 108.7, 106.7, 105.7, 105.4, 49.4, 49.0, 48.8, 39.9, 31.5, 29.6, 26.7, 25.5, 25.4, 25.3, 24.4, 24.3, 22.6, 14.0; HRMS (ESI) calcd. for C₂,H_{cs}N₂O₃ [M+H⁺] 708.4596, found 708.4606.

2-Hexanamido-N-(2-((2-(hexylcarbamoyl)-5-(piperidin-1-yl)phenyl)carbamoyl)-5-(piperidin-1-yl)phenyl)-4-(piperidin-1-yl)benzamide (4Pip₂)

Yield: 22 mg (92%). White solid; ¹H NMR (400 MHz, CDCl₂) δ 12.61 (s, 1H), 12.46 (s, 1H), 11.77 (s, 1H), 8.42 (s, 1H), 8.30 (d, J=9.6 Hz, 2H), 7.82 (dd, J=9.0, 3.0 Hz, 2H), 7.34 (d, J=8.8 Hz, 1H), 6.69 (s, 1H), 6.58 (s, 2H), 6.12 (s, 1H), 3.43–3.33 (m, 14H), 2.44 (t, J=7.5 Hz, 2H), 1.80–1.57 (m, 22H), 1.42–1.34 (m, 6H), 1.33–1.29 (m, 4H), 0.94–0.84 (m, 6H); ¹³C NMR (100 MHz, CDCl₂) δ 172.5, 169.1, 168.1, 154.2, 142.6, 141.7, 129.3, 129.0, 127.6, 109.6, 109.3, 108.9, 108.6, 106.6, 105.8, 105.6, 48.7, 39.9, 38.7, 31.5, 31.4, 29.6, 26.7, 25.4, 25.3, 25.1, 24.4, 22.6, 22.5, 14.0, 13.9; HRMS (ESI) calcd. for $C_{AB}H_{67}N_7O_ANa$ [M + Na⁺] 828.5152, found 828.5164.

N-Hexyl-2-(2-(2-(2-nitro-4-(piperidin-1-yl)benzamido)-4-(piperidin-1-yl)benzamido)-4-(piperidin-1-yl) benzamido)-4-(piperidin-1-yl)benzamide (12)

Yield: 46 mg (69%). Yellow solid; ¹H NMR (400 MHz, CDCl₂) δ 12.61 (s, 1H), 12.46 (s, 1H), 12.35 (s, 1H), 8.44 (s, 1H), 8.31 (s, 1H), 8.22 (s, 1H), 7.86 (d, J=8.9 Hz, 1H), 7.82 (d, J=9.0 Hz, 1H), 7.63 (d, J=8.7 Hz, 1H), 7.34 (d, J=8.5 Hz, 1H), 7.27 (d, J=2.5 Hz, 1H), 7.01 (dd, J=8.7, 2.4 Hz, 1H), 6.79-6.47 (m, 3H), 6.13 (s, 1H), 3.43-3.31 $(m, 18H), 1.78-1.58 (m, 26H), 1.40-1.27 (m, 6H), 0.89 (t, J = 6.9 Hz, 3H); {}^{13}C NMR (100 MHz, CDCl₂) <math>\delta$ 169.1, 168.1, 164.3, 154.1, 152.6, 150.1, 142.6, 142.4, 141.7, 129.8, 129.3, 129.0, 127.7, 120.7, 117.1, 109.8, 109.1, 106.1, 48.9, 39.9, 31.5, 29.5, 26.7, 25.3, 25.2, 24.3, 24.1, 22.6, 14.0; HRMS (ESI) calcd. for $C_{E_A}H_{E_A}N_0O_ENa$ [M+Na⁺] 962.5268, found 962.5436.

2-Amino-N-(2-((2-((2-(hexylcarbamoyl)-5-(piperidin-1-yl)phenyl)carbamoyl)-5-(piperidin-1-yl)phenyl) carbamoyl)-5-(piperidin-1-yl)phenyl)-4-(piperidin-1-yl)benzamide (13)

Yield: 24 mg (99%). White solid; ¹H NMR (400 MHz, CDCl₂) δ 12.59 (s, 1H), 12.44 (s, 1H), 12.33 (s, 1H), 8.42 (d, J=2.4 Hz, 1H), 8.34 (d, J=2.5 Hz, 1H), 8.29 (d, J=2.4 Hz, 1H), 7.85 (d, J=9.1 Hz, 1H), 7.81 (d, J=9.1 Hz, 1H),7.72 (d, J = 9.0 Hz, 1H), 7.33 (d, J = 8.9 Hz, 1H), 6.68 (dd, J = 9.0, 2.3 Hz, 1H), 6.62 (d, J = 7.5 Hz, 1H), 6.54 (dd, J = 8.8, 2.2 Hz, 1H), 6.35 (dd, J=8.9, 1.9 Hz, 1H), 6.32–6.02 (m, 2H), 6.15 (s, 2H), 3.42–3.33 (m, 14H), 3.28–3.23 (m, 4H), 1.75-1.63 (m, 26H), 1.39-1.26 (m, 6H), 0.88 (t, J=6.7 Hz, 3H); 13 C NMR (100 MHz, CDCl₂) δ 169.2, 168.3, 168.2, 168.1, 154.0, 151.4, 143.2, 142.6, 141.7, 129.7, 129.2, 128.9, 127.6, 110.2, 109.7, 109.6, 109.2, 108.7, 108.6, 106.6, 106.1, 105.9, 105.8, 105.4, 49.4, 49.0, 48.8, 39.9, 31.5, 29.7, 29.6, 26.7, 25.5, 25.4, 25.3, 24.5, 24.4, 24.3, 22.6, 14.0; HRMS (ESI) calcd. for $C_{54}H_{74}N_{10}O_{4}$ [(M+NH₄)+(-H)] 926.5894, found 926.5865.

2-Hexanamido-N-(2-((2-((2-(hexylcarbamoyl)-5-(piperidin-1-yl)phenyl)carbamoyl)-5-(piperidin-1-yl)phenyl) carbamov()-5-(piperidin-1-yl)phenyl)-4-(piperidin-1-yl)benzamide (4Pip.)

Yield: 27 mg (90%). White solid; 'H NMR (400 MHz, CDCl.) δ 12.64 (s, 1H), 12.58 (s, 1H), 12.46 (s, 1H), 11.78 (s, 1H), 8.43 (s, 1H), 8.33 (s, 2H), 8.30 (s, 1H), 7.91–7.78 (m, 3H), 7.34 (d, J=8.8 Hz, 1H), 6.77–6.52 (m, 4H), 6.13 (s, 1H), 3.48-3.27 (m, 18H), 2.45 (t, J=7.6 Hz, 2H), 1.79-1.62 (m, 28H), 1.40-1.34 (m, 6H), 1.33-1.29 (m, 4H), 0.94–0.85 (m, 6H); ¹³C NMR (100 MHz, CDCl₂) δ 172.5, 169.1, 168.2, 168.1, 154.1, 142.6, 142.6, 142.5, 141.7, 129.3, 129.3, 129.0, 127.6, 109.3, 109.1, 108.5, 106.7, 106.1, 106.1, 106.0, 105.6, 48.8, 39.9, 38.7, 31.5, 31.4, 29.7, 29.6, 26.7, 25.4, 25.1, 24.4, 22.6, 22.5, 14.0, 13.9; HRMS (ESI) calcd. for $C_{c_0}H_{s_1}N_{s_0}O_{s_1}Na[M+Na]^+$ 1030.6253, found 1030.6275.

Selective reduction of nitro groups in brominated Aa precursors (Scheme 3)

5-bromo-2-nitro-N-(pentan-3-yl)benzamide (14)

5-Bromo-2-nitrobenzoic acid (1.00 g, 4.07 mmol) was placed in a dry round bottom flask with a stir bar, and purged with Ar. Dry, Ar purged DCM (30 mL) and five drops of amine-free dry DMF were added, and the mixture was cooled in a dry ice/acetone bath. While stirring, oxalyl chloride (700 µL, 8.1 mmol) was added dropwise and allowed to react for 30 min. The progress of the reaction was monitored using TLC, i.e. a drop of the reaction was quenched with dry methanol to form methyl ester that has a distinctly different retention factor, R_0 from the starting material. After the completion of the reaction, the mixture was concentrated, resuspended in dry DCM (25 mL) and concentrated again. This resuspending and drying was repeated three times. Under argon, the dried mixture was dissolved in dry DCM (25 mL) and cooled in a dry ice/acetone bath. While stirring, 3-aminopentane (1.4 mL, 12 mmol) was added dropwise, followed by a dropwise addition of NMM (2.2 mL, 20.3 mmol). The reaction was allowed to reach room temperature and stirred for 3 h. The mixture was diluted with 5 % HCl and stirred for additional 10 min. The resulting mixture was extracted with DCM (3×50 mL). The organic layers were collected, combined, dried over Na₂SO₄, and condensed. The resulting residue was dissolved in small amount of DMF, added to deionized water and filtered. The filtrate was diluted further with deionized water and extracted with DCM (3×25 mL). The organic layers were combined and dried over Na, SO₄. The solvent was evaporated in vacuo to afforded 1.1 g (84%) of 14 as a white solid. ¹H NMR (600 MHz, CDCl₂) δ /ppm: 7.94 (d, J=8.7 Hz, 1H), 7.69 (dd, J=8.7, 2.2 Hz, 1H), 7.61 (d, J=2.1 Hz, 1H), 5.57 (d, J=9.1 Hz, 2H), 4.02–3.93 (m, 1H), 1.72–1.62 (m, 3H), 1.56–1.50 (m, 3H), 1.01 (t, J=7.5 Hz, 6H). ¹³C NMR $(101 \text{ MHz}, \text{CDCl}_3) \delta/\text{ppm}: 164.69, 145.09, 135.05, 133.34, 131.80, 128.65, 126.10, 53.19, 27.15, 10.23. HRMS (ESI) <math>m/z$ calcd. for $C_{12}H_{16}BrN_2O_2^+$: 315.0344 [M+H]+, found 315.0216.

2-amino-5-bromo-N-(pentan-3-yl)benzamide (15)

Procedure 1: reducing with HSiCl, (i, Scheme 3)

14 (79 mg, 0.25 mmol), was transferred to a dry, argon-purged 25 mL round bottom flask with a stir bar. Dry acetonitrile (MeCN) (5 mL) was added while purging with argon, followed by followed by the addition of DIPEA (218 µL, 1.25 mmol). This solution was placed into a 0 °C ice bath and stirred for 5 min. A solution of HSiCl₂ (91 µL, 0.9 mmol) in 2 mL MeCN was prepared separately under Ar, and added to the reaction mixture dropwise over the course of 10 min. The reaction was taken out of the ice bath and stirred overnight at room temperature. The progress of the reaction was monitored using TLC. The mixture was added to 50 mL of aqueous saturated solution of NaHCO₂ and extracted with DCM (3×25 mL). The organic layers were collected, combined and dried over Na, SO,. The solvent was evaporated in vauco and recrystallized from hexanes afforded afford 29 mg (0.10 mmol, 41 % yield) of **15** as a white solid. H NMR (600 MHz, CDCl₃) δ /ppm: 7.38 (d, J=2.3 Hz, 1H), 7.26 (dd, J=8.7, 2.3 Hz, 1H), 6.57 (d, J=8.7 Hz, 1H), 5.70-5.66 (m, 1H), 5.48 (s, 2H), 3.97-3.89 (m, 1H), 1.64 (dtd, J = 14.8, 7.4, 5.4 Hz, 2H), 1.47 (dt, J = 13.9, 7.5 Hz, 2H), 0.95 (t, J = 7.4 Hz, 6H). ¹³C NMR (101 MHz, 12.8)

CDCl₂) δ /ppm: 167.82, 147.43, 134.68, 129.32, 118.92, 118.43, 107.75, 52.29, 27.54, 10.38. HRMS (ESI) m/z calcd. for C., H., BrN, O-: 283.0451 [M]-, found 283.0282.

Procedure 2: reducing with Na₂S₂O₄ (ii, Scheme 3)

14 (100 mg, 0.32 mmol), Na,S,O, (1.1 g, 6.37 mmol), K,CO, (1.23 g, 8.9 mmol), and 1,1-diheptyl-4,4-bipyridinium dibromide (442 mg, 0.857 mmol) were placed in a dry, argon-purged 25 mL round bottom flask with a stir bar. An argon-purged mixture of 5 mL DCM and 5 mL deionized water were added, and the reaction was stirred at room temperature for 2.5 h. The instant color change of the DCM phase was an indication for the formation of the viologen radical cation. The progress of the reaction in the organic phase was monitored using TLC. The mixture was added to 50 mL saturated aqueous solution of Na₂CO₂ and extracted with DCM (3×25 mL). The organic layers were collected, combined and dried over Na, SO₆. The solvent was evaporated in vacuo and recrystallized from hexanes afforded afford 58 mg (0.20 mmol, 64 % yield) of 15 as a white solid.

Procedure 3: reducing with CrCl, (iii, Scheme 3)

This reaction was performed in a glovebox filled with argon (0,<1 ppm, H,0<1 ppm). 14 (50 mg, 0.16 mmol) and CrCl₂ (310 mg, 2.5 mmol) were dissolved in 5 mL of argon purged dry DMF and transferred to a dry 100 mL round bottom flask with a stir bar. The solution was stirred for 4 h and the progress was monitored using TLC. Upon completion, the mixture was taken out of the glove box, added to 100 mL of aqueous EDTA solution (0.03 M) and extracted with ethyl acetate (3×25 mL). The organic layers were collected, combined, and dried over Na₂SO₆. The solvent was evaporated *in vacuo* and recrystallized from hexanes afforded afford 43 mg (0.15 mmol, 95 % yield) of 15 as a white solid.

Optical absorption and emission spectroscopy

Steady-state absorption spectra were recorded in a transmission mode using a JASCO V-670 spectrophotometer (Tokyo, Japan); and steady-state emission spectra were measured, also in a transmission mode, with a FluoroLog-3 spectrofluorometer (Horiba-Jobin-Yvon, Edison, NJ, USA) as previously reported [179]. The reported fluorescence spectra, $F(\tilde{\nu})$, were obtained from the fluorescence spectra, $F(\lambda)$, recorded vs. wavelength, i.e. $F(\tilde{\nu}) = F(\lambda) \lambda^2$.

Electrochemical analysis

Cyclic voltammetry is conducted using Reference 600 Potentiostat/Galvanostat/ZRA (Gamry Instruments, PA, USA), connected to a three-electrode cell, at scan rates of 50 mV s⁻¹, as previously described [177, 178]. Anhydrous solvents are employed for the sample preparation, with different concentrations of tetrabutylammonium hexafluorophosphate, $N(n-C_hH_o)_hPF_o$, as supporting electrolyte. Prior to recording the voltammograms, the samples are extensively purged with argon while maintaining constant volume by adding more of the anhydrous solvent. For each sample and each solvent, a set of voltammograms is recorded where the electrolyte concentration is increased from 25 mM to 200 mM in increments of 25 mM. The half-wave potentials, $E^{(1/2)}$, are determined from the first inflection point of the anodic waves, i.e. the potentials where $\partial^2 I/\partial E^2 = 0$ at $\partial E/\partial t = \text{constant}$ [55, 176]. To correct for potential drifts in the reference electrode (which is SCE, connected with the cell via a salt bridge), ferrocene was used as a standard, i.e. $E^{(1/2)} = 0.45 \pm 0.01$ V vs. SCE for MeCN, 100 mM $N(n-C_aH_o)_aBF_a$ [177]. Voltammograms of the standard are recorded before and after each set of measurements. From the dependence of $E^{(1/2)}$ on the electrolyte concentration (Fig. 5b), the potential for neat solvents are estimated from extrapolation to zero electrolyte concentration [180].

Supplementary material

The online version of this article offers supplementary material, i.e. ¹H and ¹³C NMR spectra of the products and the key intermediates, available to authorized users.

Acknowledgments: Funding for this work was from the USA National Science Foundation, Funder Id: http:// dx.doi.org/10.13039/100000165, grants CHE 1465284 and CHE 1800602.

References

- [1] V. I. Vullev. I. Phys. Chem. Lett. 2, 503 (2011).
- [2] J. J. Warren, J. R. Winkler, H. B. Gray. Coord. Chem. Rev. 257, 165 (2013).
- [3] U. Brandt. BIOspektrum 20, 267 (2014).
- [4] R. M. Metzger. Chem. Rev. 115, 5056 (2015).
- [5] J. B. Derr, J. Tamayo, E. M. Espinoza, J. A. Clark, V. I. Vullev. Can. J. Chem. 96, 843 (2018).
- [6] S. Ilic, A. Alherz, C. B. Musgrave, K. D. Glusac. Chem. Soc. Rev. 47, 2809 (2018).
- [7] A. Purc, E. M. Espinoza, R. Nazir, J. J. Romero, K. Skonieczny, A. Jeżewski, J. M. Larsen, D. T. Gryko, V. I. Vullev. J. Am. Chem. Soc. 138, 12826 (2016).
- [8] E. M. Espinoza, J. M. Larsen-Clinton, M. Krzeszewski, N. Darabedian, D. T. Gryko, V. I. Vullev. Pure Appl. Chem. 89, 1777 (2017).
- [9] R. Breslow. Chem. Soc. Rev. 1, 553 (1972).
- [10] C. A. Scherer, C. A. Dorschel, J. M. Cook, P. W. Le Quesne. J. Org. Chem. 37, 1083 (1972).
- [11] E. Leete. J. Chem. Soc., Chem. Commun. 1091 (1972).
- [12] S. M. Kupchan, R. M. Schubert. Science 185, 791 (1974).
- [13] R. Y. Tam, L. J. Smith, M. S. Shoichet. Acc. Chem. Res. 50, 703 (2017).
- [14] T. T. Teeri, H. Brumer, G. Daniel, P. Gatenholm. Trends Biotechnol. 25, 299 (2007).
- [15] X. Chen, G. S. Lee, A. Zettl, C. R. Bertozzi. Angew. Chem., Int. Ed. 43, 6111 (2004).
- [16] G. Tempesti, D. Mange, A. Stauffer. Riv. Biol. 92, 143 (1999).
- [17] A. Rosas. J. Med. 45, 173 (1961).
- [18] J. S. Moya Corral. Rev. R. Acad. Cienc. Exactas, Fis. Nat. 90, 97 (1996).
- [19] T. Aida, D.-L. Jiang, M.-S. Choi, M. Enomoto. Polym. Mater. Sci. Eng. 80, 257 (1999).
- [20] A. E. Barron, R. N. Zuckermann. Curr. Opin. Chem. Biol. 3, 681 (1999).
- [21] M. Enomoto, T. Aida. Yuki Gosei Kagaku Kyokaishi 57, 924 (1999).
- [22] A. Mandel, W. Schmitt, T. G. Womack, R. Bhalla, R. K. Henderson, S. L. Heath, A. K. Powell. Coord. Chem. Rev. 190-192, 1067 (1999).
- [23] Z. Hu, R. D. Williams, D. Tran, T. G. Spiro, S. M. Gorun. J. Am. Chem. Soc. 122, 3556 (2000).
- [24] M. K. Brennaman, R. J. Dillon, L. Alibabaei, M. K. Gish, C. J. Dares, D. L. Ashford, R. L. House, G. J. Meyer, J. M. Papanikolas, T. J. Meyer. J. Am. Chem. Soc. 138, 13085 (2016).
- [25] E. L. Efurumibe, A. D. Asiegbu. Int. J. Phys. Sci. 8, 2053 (2013).
- [26] D. G. Nocera. Acc. Chem. Res. 45, 767 (2012).
- [27] J. Kim, I. Jeerapan, J. R. Sempionatto, A. Barfidokht, R. K. Mishra, A. S. Campbell, L. J. Hubble, J. Wang. Acc. Chem. Res. 51,
- [28] N. Mano, A. de Poulpiquet. Chem. Rev. 118, 2392 (2018).
- [29] R. M. Evans, B. Siritanaratkul, C. F. Megarity, K. Pandey, T. F. Esterle, S. Badiani, F. A. Armstrong. Chem. Soc. Rev. 48, 2039 (2019).
- [30] M. del Barrio, M. Sensi, C. Orain, C. Baffert, S. Dementin, V. Fourmond, C. Leger. Acc. Chem. Res. 51, 769 (2018).
- [31] L. Hammarstroem. Acc. Chem. Res. 48, 840 (2015).
- [32] D. L. Ashford, M. K. Gish, A. K. Vannucci, M. K. Brennaman, J. L. Templeton, J. M. Papanikolas, T. J. Meyer. Chem. Rev. 115, 13006 (2015).
- [33] R. A. Marcus. Disc. Faraday Soc. 21 (1960).
- [34] S. Yomosa. Sup. Prog. Theor. Phys. 249 (1967).
- [35] S. G. Boxer. Annu. Rev. Biophys. Biophys. Chem. 19, 267 (1990).
- [36] W. G. J. Hol, P. T. Van Duijnen, H. J. C. Berendsen. Nature 273, 443 (1978).
- [37] A. Wada. J. Chem. Phys. 30, 328 (1959).
- [38] Y.-G. K. Shin, M. D. Newton, S. S. Isied. J. Am. Chem. Soc. 125, 3722 (2003).

- [39] E. Galoppini, M. A. Fox. J. Am. Chem. Soc. 118, 2299 (1996).
- [40] S. Yasutomi, T. Morita, Y. Imanishi, S. Kimura. Science 304, 1944 (2004).
- [41] L. Garbuio, S. Antonello, I. Guryanov, Y. J. Li, M. Ruzzi, N. J. Turro, F. Maran. J. Am. Chem. Soc. 134, 10628 (2012).
- [42] C. Shlizerman, A. Atanassov, I. Berkovich, G. Ashkenasy, N. Ashkenasy. J. Am. Chem. Soc. 132, 5070 (2010).
- [43] M. Lauz, S. Eckhardt, K. M. Fromm, B. Giese. Phys. Chem. Chem. Phys. 14, 13785 (2012).
- [44] H. B. Gray, J. R. Winkler. Proc. Natl. Acad. Sci. U.S.A. 102, 3534 (2005).
- [45] V. I. Vullev, G. Jones II. Res. Chem. Intermed. 28, 795 (2002).
- [46] G. Jones II, X. Zhou, V. I. Vullev. Photochem. Photobiol. Sci. 2, 1080 (2003).
- [47] F. D. Lewis, Isr. I. Chem. 53, 350 (2013).
- [48] R. Venkatramani, S. Keinan, A. Balaeff, D. N. Beratan. Coord. Chem. Rev. 255, 635 (2011).
- [49] E. Wierzbinski, A. de Leon, X. Yin, A. Balaeff, K. L. Davis, S. Rapireddy, R. Venkatramani, S. Keinan, D. H. Ly, M. Madrid, D. N. Beratan, C. Achim, D. H. Waldeck. J. Am. Chem. Soc. 134, 9335 (2012).
- [50] M. K. Ashraf, R. R. Pandey, R. K. Lake, B. Millare, A. A. Gerasimenko, D. Bao, V. I. Vullev. Biotechnol. Prog. 25, 915 (2009).
- [51] B. Xia, D. Bao, S. Upadhyayula, G. Jones, V. I. Vullev. J. Org. Chem. 78, 1994 (2013).
- [52] D. Bao, S. Upadhyayula, J. M. Larsen, B. Xia, B. Georgieva, V. Nunez, E. M. Espinoza, J. D. Hartman, M. Wurch, A. Chang, C.-K. Lin, J. Larkin, K. Vasquez, G. J. O. Beran, V. I. Vullev. J. Am. Chem. Soc. 136, 12966 (2014).
- [53] J. M. Larsen, E. M. Espinoza, V. I. Vullev. J. Photon. Energy. 5, 055598 (2015).
- [54] M. Krzeszewski, E. M. Espinoza, C. Cervinka, J. B. Derr, J. A. Clark, D. Borchardt, G. J. O. Beran, D. T. Gryko, V. I. Vullev. Angew. Chem., Int. Ed. 57, 12365 (2018).
- [55] E. M. Espinoza, J. M. Larsen, V. I. Vullev. J. Phys. Chem. Lett. 7, 758 (2016).
- [56] J. M. Larsen, E. M. Espinoza, J. D. Hartman, C.-K. Lin, M. Wurch, P. Maheshwari, R. K. Kaushal, M. J. Marsella, G. J. O. Beran, V. I. Vullev. Pure Appl. Chem. 87, 779 (2015).
- [57] J. M. Larsen-Clinton, E. M. Espinoza, M. F. Mayther, J. Clark, C. Tao, D. Bao, C. M. Larino, M. Wurch, S. Lara, V. I. Vullev. Phys. Chem. Chem. Phys. 19, 7871 (2017).
- [58] H. Meyer. Justus Liebigs Ann. Chem. 351, 267 (1907).
- [59] K. Butler, M. W. Partridge. J. Chem. Soc. 2396 (1959).
- [60] A. Hoorfar, W. D. Ollis, J. F. Stoddart, D. J. Williams. Tetrahedron Lett. 21, 4211 (1980).
- [61] A. Hoofar, W. D. Ollis, J. F. Stoddart. J. Chem. Soc., Perkin Trans. 1, 1721 (1982).
- [62] W. D. Ollis, J. F. Stoddart. Inclusion Compd. 2, 169 (1984).
- [63] K. Imagawa, H. Tsuneyuki, S. Miyata, T. Oda, K. Nishino, Y. Ikutani. Osaka Kyoiku Daigaku Kiyo, Dai-3-bumon 36, 123 (1987).
- [64] Y. Hamuro, S. J. Geib, A. D. Hamilton. J. Am. Chem. Soc. 118, 7529 (1996).
- [65] A. Varnavas, L. Lassiani, V. Valenta. Farmaco 55, 369 (2000).
- [66] A. Varnavas, V. Valenta, F. Berti, L. Lassiani. Farmaco 56, 555 (2001).
- [67] T. Minami, S. Koyamoto, M. Kobayashi, R. Tanaka, Y. Hatanaka. Chem. Lett. 34, 434 (2005).
- [68] R. V. Nair, S. Kheria, S. Rayavarapu, A. S. Kotmale, B. Jagadeesh, R. G. Gonnade, V. G. Puranik, P. R. Rajamohanan, G. J. Sanjayan. J. Am. Chem. Soc. 135, 11477 (2013).
- [69] K. J. Wilson, J. Xiao, C. Z. Chen, Z. Huang, I. U. Agoulnik, M. Ferrer, N. Southall, X. Hu, W. Zheng, X. Xu, A. Wang, C. Myhr, E. Barnaeva, E. R. George, A. I. Agoulnik, J. J. Marugan. Eur. J. Med. Chem. 156, 79 (2018).
- [70] S. Krauthaeuser, L. A. Christianson, D. R. Powell, S. H. Gellman. J. Am. Chem. Soc. 119, 11719 (1997).
- [71] Y. Hamuro, A. D. Hamilton. Bioorg. Med. Chem. 9, 2355 (2001).
- [72] M. W. Giuliano, W. S. Horne, S. H. Gellman. J. Am. Chem. Soc. 131, 9860 (2009).
- [73] E. M. Espinoza, V. I. Vullev. ECS Trans. 77, 1517 (2017).
- [74] E. M. Espinoza, J. M. Larsen, V. I. Vullev. ECS Trans. 66, 1 (2015).
- [75] E. M. Espinoza, D. Bao, M. Krzeszewski, D. T. Gryko, V. I. Vullev. Int. J. Chem. Kinet. Ahead of Print (2019).
- [76] E. Fischer, E. Fourneau. Ber. Dtsch. chem. Ges. 34, 2868 (1901).
- [77] V. du Vigneaud, C. Ressler, J. M. Swan, C. W. Roberts, P. G. Katsoyannis. J. Am. Chem. Soc. 76, 3115 (1954).
- [78] P. G. Katsoyannis. J. Polym. Sci. 49, 51 (1961).
- [79] J. Meienhofer, E. Schnabel, H. Bremer, O. Brinkhoff, R. Zabel, W. Sroka, H. Klostermeyer, D. Brandenburg, T. Okuda, H. Zahn. Z. Naturforsch. 18b, 1120 (1963).
- [80] P. G. Katsoyannis, A. Tometsko, K. Fukuda. J. Am. Chem. Soc. 85, 2863 (1963).
- [81] Y.-T. Kung, Y.-C. Du, W.-T. Huang, C.-C. Chen, L.-T. Ke, S.-C. Hu, R.-Q. Jiang, S.-Q. Chu, C.-I. Niu, J.-Z. Hsu, W.-C. Chang, L.-L. Chen, H.-S. Li, Y. Wang, T.-P. Loh, A.-H. Chi, C.-H. Li, P.-T. Shi, Y.-H. Yieh, K.-L. Tang, C.-Y. Hsing. Sci. Sin. 14, 1710 (1965).
- [82] Y. Pan, Y. Tu, W. Hawan, C. Chen, L. Go. Tanpakushitsu Kakusan Koso 11, 603 (1966).
- [83] Y.-T. Kung, Y.-C. Du, W.-T. Huang, C.-C. Chen, L.-T. Ke, S.-C. Hu, R.-Q. Jiang, S.-Q. Chu, C.-I. Niu, J.-Z. Hsu, W.-C. Chang, L.-L. Chen, H.-S. Li, Y. Wang, T.-P. Loh, A.-H. Chi, C.-H. Li, P.-T. Shi, Y.-H. Yieh, K.-L. Tang, C.-Y. Hsing. Sci. Sin. 15, 544 (1966).
- [84] H. Zahn. Naturwissenschaften 54, 396 (1967).
- [85] H. Zahn, G. Schmidt. Tetrahedron Lett. 5095 (1967).
- [86] R. B. Merrifield. J. Am. Chem. Soc. 85, 2149 (1963).

- [87] L. A. Carpino, G. Y. Han. J. Am. Chem. Soc. 92, 5748 (1970).
- [88] L. A. Carpino, G. Y. Han. J. Org. Chem. 37, 3404 (1972).
- [89] M. Stawikowski, G. B. Fields. Curr. Protoc. Protein. Sci. Chapter 18, Unit 18 1 (2012).
- [90] G. R. Marshall. Amino Acids, Pept. Proteins Org. Chem. 3, 253 (2011).
- [91] F. D. Bellamy, K. Ou. Tetrahedron Lett. 25, 839 (1984).
- [92] D. Formenti, F. Ferretti, F. K. Scharnagl, M. Beller. Chem. Rev. 119, 2611 (2019).
- [93] A. M. Tafesh, J. Weiguny. Chem. Rev. 96, 2035 (1996).
- [94] M. Orlandi, D. Brenna, R. Harms, S. Jost, M. Benaglia. Org. Process Res. Dev. 22, 430 (2018).
- [95] Y. N. A. Harari. Sapiens: A Brief history of Humankind. First U.S. edition. Harper, New York (2015).
- [96] S. Gupta, M. R. Chatni, A. L. N. Rao, V. I. Vullev, L. V. Wang, B. Anvari. Nanoscale 5, 1772 (2013).
- [97] B. Bahmani, Y. Guerrero, D. Bacon, V. Kundra, V. I. Vullev, B. Anvari. Lasers Surg Med 46, 582 (2014).
- [98] J. Wan, M. S. Thomas, S. Guthrie, V. I. Vullev. Ann. Biomed. Eng. 37, 1190 (2009).
- [99] G. M. Whitesides. Nature 442, 368 (2006).
- [100] M. S. Thomas, B. Millare, J. M. Clift, D. Bao, C. Hong, V. I. Vullev. Ann Biomed Eng 38, 21 (2010).
- [101] K. Chau, B. Millare, A. Lin, S. Upadhyayula, V. Nuñez, H. Xu, V. I. Vullev. Microfluid. Nanofluid. 10, 907 (2011).
- [102] J. H. Sung, Y. I. Wang, N. Narasimhan Sriram, M. Jackson, C. Long, J. J. Hickman, M. L. Shuler. Anal. Chem. 91, 330 (2019).
- [103] E. Cinar, S. Zhou, J. DeCourcey, Y. Wang, R. E. Waugh, J. Wan. Proc. Natl. Acad. Sci. U.S.A. 112, 11783 (2015).
- [104] A. M. Forsyth, J. Wan, P. D. Owrutsky, M. Abkarian, H. A. Stone. Proc. Natl. Acad. Sci. U.S.A. 108, 10986 (2011).
- [105] S. K. Y. Tang, W. F. Marshall. Science 356, 1022 (2017).
- [106] T. Yamashita, K. Abe. Curr. Pharm. Des. 18, 3649 (2012).
- [107] S. Kuang, M. A. Rudnicki. Trends Mol. Med. 14, 82 (2008).
- [108] S. Pekovic, S. Subasic, N. Nedeljkovic, I. Bjelobaba, R. Filipovic, I. Milenkovic. "Molecular basis of brain injury and repair", in Neurobiological Studies-From Genes to Behaviour, S. Ruzdijic, L. Rakic (Eds.), pp. 143-165, Research Signpost, India (2006).
- [109] P. A. Beachy, S. S. Karhadkar, D. M. Berman. Nature 432, 324 (2004).
- [110] R. Yatsunami, S. Nakamura. Kagaku to Kyoiku 49, 122 (2001).
- [111] M. Krzeszewski, T. Kodama, E. M. Espinoza, V. I. Vullev, T. Kubo, D. T. Gryko. Chem. Eur. J. 22, 16478 (2016).
- [112] K. Skonieczny, J. Yoo, J. M. Larsen, E. M. Espinoza, M. Barbasiewicz, V. I. Vullev, C.-H. Lee, D. T. Gryko. Chem. Eur. J. 22, 7485 (2016).
- [113] A. J. Wierzba, A. Wincenciuk, M. Karczewski, V. I. Vullev, D. Gryko. Chem. Eur. J. 24, 10344 (2018).
- [114] J. A. Warren. MRS Bull. 43, 452 (2018).
- [115] Z. Liu, Y. Li, D. Shi, Y. Guo, M. Li, X. Zhou, Q. Huang, S. Du. Scr. Mater. 141, 99 (2017).
- [116] M. R. Norman. Rep. Prog. Phys. 79, 074502/1 (2016).
- [117] A. W. Bosse, E. K. Lin. J. Polym. Sci., Part B Polym. Phys. 53, 89 (2015).
- [118] L. Kaufman, J. Agren. Scr. Mater. 70, 3 (2014).
- [119] W. R. Entley, G. S. Girolami. Science 268, 397 (1995).
- [120] S. Bertaina, S. Gambarelli, T. Mitra, B. Tsukerblat, A. Mueller, B. Barbara. Nature 453, 203 (2008).
- [121] L. Bogani, W. Wernsdorfer. Nat. Mater. 7, 179 (2008).
- [122] S. Upadhyayula, D. Bao, B. Millare, S. S. Sylvia, K. M. M. Habib, K. Ashraf, A. Ferreira, S. Bishop, R. Bonderer, S. Baqai, X. Jing, M. Penchev, M. Ozkan, C. S. Ozkan, R. K. Lake, V. I. Vullev. J. Phys. Chem. B 115, 9473 (2011).
- [123] J. Li, Y. Wang, J. Chen, Z. Liu, A. Bax, L. Yao. J. Am. Chem. Soc. 138, 1824 (2016).
- [124] E. M. Espinoza, J. A. Clark, J. B. Derr, D. Bao, B. Georgieva, F. H. Quina, V. I. Vullev. ACS Omega 3, 12857 (2018).
- [125] H.-M. Huang, H. Kries. *Biochemistry* **58**, 73 (2019).
- [126] H. Lundberg, F. Tinnis, N. Selander, H. Adolfsson. Chem. Soc. Rev. 43, 2714 (2014).
- [127] I. Coin, M. Beyermann, M. Bienert. Nat. Protoc. 2, 3247 (2007).
- [128] W. Klee, M. Breener. Helv. Chim. Acta 44, 2151 (1950).
- [129] G. W. Anderson, R. Paul. J. Am. Chem. Soc. 80, 4423 (1958).
- [130] F. Albericio. Biopolymers 55, 123 (2000).
- [131] C. A. G. N. Montalbetti, V. Falque. Tetrahedron 61, 10827 (2005).
- [132] E. Valeur, M. Bradley. Chem. Soc. Rev. 38, 606 (2009).
- [133] R. B. Merrifield. Chem. Polypeptides, 335 (1973).
- [134] E. Robinson Noah, B. Robinson Arthur. Biopolymers 90, 297 (2008).
- [135] R. Behrendt, P. White, J. Offer. J. Pept. Sci. 22, 4 (2016).
- [136] V. Made, S. Els-Heindl, G. Beck-Sickinger Annette. Beilstein. J. Org. Chem. 10, 1197 (2014).
- [137] H.-A. Klok. Highlights Bioorg. Chem. 554 (2004).
- [138] C. Fromont, V. Pomel, M. Bradley. Integr. Drug Discovery Technol. 463 (2002).
- [139] S. Okamoto, T. Morita, S. Kimura. Langmuir 25, 3297 (2009).
- [140] K. Kitagawa, T. Morita, S. Kimura. Langmuir 21, 10624 (2005).
- [141] V. I. Vullev, G. Jones. Tetrahedron Lett. 43, 8611 (2002).
- [142] G. Jones II, V. I. Vullev. Org. Lett. 4, 4001 (2002).

- [143] G. Jones II, V. Vullev, E. H. Braswell, D. Zhu. J. Am. Chem. Soc. 122, 388 (2000).
- [144] M. A. Fox, E. Galoppini. J. Am. Chem. Soc. 119, 5277 (1997).
- [145] G. Jones II, L. N. Lu, V. Vullev, D. Gosztola, S. Greenfield, M. Wasielewski. Bioorg. Med. Chem. Lett. 5, 2385 (1995).
- [146] S. E. Allen, S.-Y. Hsieh, O. Gutierrez, J. W. Bode, M. C. Kozlowski. J. Am. Chem. Soc. 136, 11783 (2014).
- [147] S. L. Pedersen, A. P. Tofteng, L. Malik, K. J. Jensen. Chem. Soc. Rev. 41, 1826 (2012).
- [148] G. Sabatino, A. M. Papini. Curr. Opin. Drug Discovery Dev. 11, 762 (2008).
- [149] M. Bodanszky, J. Martinez. Synthesis 333 (1981). DOI: 10.1055/s-1981-29442.
- [150] B. F. Gisin, R. B. Merrifield. J. Am. Chem. Soc. 94, 3102 (1972).
- [151] P. B. Harbury, T. Zhang, P. S. Kim, T. Alber. Science 262, 1401 (1993).
- [152] K. J. Lumb, P. S. Kim. Science 268, 436 (1995).
- [153] G. Jones II, V. I. Vullev. Org. Lett. 3, 2457 (2001).
- [154] G. Jones II, V. I. Vullev. J. Phys. Chem. A 105, 6402 (2001).
- [155] P. Verdie, G. Subra, M.-C. Averland-Petit, M. Amblard, J. Martinez. J. Comb. Chem. 10, 869 (2008).
- [156] M.-K. Jeon, H. J. La, D.-C. Ha, Y.-D. Gong. Synlett, 1431 (2007). DOI: 10.1055/s-2007-980368.
- [157] M.-K. leon, M.-S. Kim, I.-I. Kwon, Y.-D. Gong, D.-H. Lee, *Tetrahedron* **64**, 9060 (2008).
- [158] H.-Y. Lee, M. An. Bull. Korean Chem. Soc. 25, 1717 (2004).
- [159] M. Orlandi, F. Tosi, M. Bonsignore, M. Benaglia. Org. Lett. 17, 3941 (2015).
- [160] M. Orlandi, M. Benaglia, F. Tosi, R. Annunziata, F. Cozzi. J. Org. Chem. 81, 3037 (2016).
- [161] N. J. Blackburn, R. W. Strange, R. T. Carr, S. J. Benkovic. *Biochemistry* 31, 5298 (1992).
- [162] D. R. Davydov, H. Fernando, B. J. Baas, S. G. Sligar, J. R. Halpert. Biochemistry 44, 13902 (2005).
- [163] B. Bahmani, S. Gupta, S. Upadhyayula, V. I. Vullev, B. Anvari. J. Biomed. Opt. 16, 051303/1 (2011).
- [164] A. Decken, S. Greer, F. Grein, A. Mailman, B. Mueller, T. A. P. Paulose, J. Passmore, J. M. Rautiainen, S. A. Richardson, M. J. Schriver, T. K. Whidden. Inorg. Chem. 55, 5999 (2016).
- [165] S. M. Lough, J. W. McDonald. Inorg. Chem. 26, 2024 (1987).
- [166] W. C. Hodgeman, J. B. Weinrach, D. W. Bennett. Inorg. Chem. 30, 1611 (1991).
- [167] E. Boll, H. Drobecq, N. Ollivier, L. Raibaut, R. Desmet, J. Vicogne, O. Melnyk. Chem. Sci. 5, 2017 (2014).
- [168] R. Kaplanek, V. Krchnak. Tetrahedron Lett. 54, 2600 (2013).
- [169] E. Schütznerová, V. Krchňák. ACS Comb. Sci. 17, 137 (2015).
- [170] I. Messina, I. Popa, V. Maier, M. Soural. ACS Comb. Sci. 16, 33 (2014).
- [171] C. McMaster, V. Fulopova, I. Popa, M. Grepl, M. Soural. ACS Comb. Sci. 16, 221 (2014).
- [172] R. A. Scheuerman, D. Tumelty. Tetrahedron Lett. 41, 6531 (2000).
- [173] A. Hari, B. L. Miller. Tetrahedron Lett. 40, 245 (1999).
- [174] A. Hari, B. L. Miller. Angew. Chem., Int. Ed. 38, 2777 (1999).
- [175] A. Hari, B. L. Miller. Org. Lett. 2, 691 (2000).
- [176] E. M. Espinoza, J. A. Clark, J. Soliman, J. B. Derr, M. Morales, V. I. Vullev. J. Electrochem. Soc. 166, H3175 (2019).
- [177] D. Bao, B. Millare, W. Xia, B. G. Steyer, A. A. Gerasimenko, A. Ferreira, A. Contreras, V. I. Vullev. J. Phys. Chem. A 113, 1259 (2009).
- [178] D. Bao, S. Ramu, A. Contreras, S. Upadhyayula, J. M. Vasquez, G. Beran, V. I. Vullev. J. Phys. Chem. B 114, 14467 (2010).
- [179] S. Upadhyayula, V. Nunez, E. M. Espinoza, J. M. Larsen, D. Bao, D. Shi, J. T. Mac, B. Anvari, V. I. Vullev. Chem. Sci. 6, 2237
- [180] E. M. Espinoza, B. Xia, N. Darabedian, J. M. Larsen, V. Nunez, D. Bao, J. T. Mac, F. Botero, M. Wurch, F. Zhou, V. I. Vullev. Eur. J. Org. Chem. 2016, 343 (2016).

Supplementary Material: The online version of this article offers supplementary material (https://doi.org/10.1515/pac-2019-0111).